ESTIMATING ATTENUATION PROPERTIES OF BENTONITE LAYER IN CUT BANK OIL FIELD, GLACIER COUNTY, MONTANA

A Thesis

by

NECDET KARAKURT

Submitted to the Office of Graduate Studies of
Texas A&M University
in partial fulfillment of the requirements for the degree of

MASTER OF SCIENCE

December 2005

Major Subject: Geophysics

ESTIMATING ATTENUATION PROPERTIES OF BENTONITE LAYER IN CUT BANK OIL FIELD, GLACIER COUNTY, MONTANA

A Thesis

by

NECDET KARAKURT

Submitted to the Office of Graduate Studies of
Texas A&M University
in partial fulfillment of the requirements for the degree of

MASTER OF SCIENCE

Approved by:

Chair of Committee,	Richard L. Gibson
Committee Members,	Steven L. Dorobek
	Joel S. Watkins
	Duane A. McVay
Head of Department,	Richard Carlson

December 2005

Major Subject: Geophysics

ABSTRACT

Estimating Attenuation Properties of Bentonite Layer in Cut Bank Oil Field, Glacier County, Montana. (December 2005)
Necdet Karakurt, B.S., Istanbul Technical University
Chair of Advisory Committee: Dr. Richard L. Gibson

Acquisition and interpretation of 3-D seismic data led DeAngelo and Hardage (2001) to describe the channel system in the south central Cut Bank area in Glacier County, Montana. The presence of a low velocity layer called Bentonite was also discovered in the area with the help of well-logs. Bentonite is a volcanic ash, which lies on both sides of the channel system and is absent within the channel. DeAngelo and Hardage (2001) shot a vertical seismic profiling (VSP) survey at well # 54-8 to analyze the formation structure in depth, since seismic signals around the reservoir area were unclear in the 3-D survey.

This research attempts to estimate the attenuation properties of the Bentonite layer in the Cut Bank oil field. VSP data is processed for velocity information and estimation of seismic Q using the spectral ratios method (SRM). The SRM theoretically assumes that the propagating signal is a plane seismic wave traveling vertically from one point to another in a homogeneous model. The amplitudes at the start and end points are known and relate to each other with the attenuation coefficient in a frequency range. The relation between the seismic amplitudes at z distance from each other can be expressed as a linear function of frequency after a few modifications. SRM uses the linearity of the logarithmic ratio of the seismic amplitudes over a frequency range. In theory, ratios plotted against a frequency range must produce a flat line. However, in practice, the logarithmic ratios are expected to draw an approximate line (curve), where some of the data points deviate from the origin of the line. Thus fitting a line to the ratios curve and calculating the slope of this curve are necessary. Slope of the curve relates to the seismic attenuation coefficient and further to the seismic Q.

The SRM results suggest that Bentonite may have a Q value as low as 5. This highly attenuative and thin (20 to 40 $feet$ throughout the south central Cut Bank Unit) layer alters seismic signals propagating through it. A thorough analysis of the amplitude spectra suggests that seismic signals dramatically lose their energy when they pass through Bentonite. Low energy content of the signals below the

Bentonite layer highlights that the recovery of the seismic energy is less likely despite the presence of multiples, which are known to affect the seismic signals constructively. Therefore, separation of reflected events is a greater challenge for the thin reservoir sand units lying underneath the Bentonite layer. Thus the Bentonite layer in the Cut Bank oil field has to be taken seriously and data processing should be done accordingly for better accuracy.

DEDICATION

To my parents, Ishak and Emine Karakurt,
my brother, Dr. Ismail Karakurt,
my sisters Hatice Albayrak and Sakine Deniz,
my brother in laws, nephews, nieces and relatives,
and my wife, Norma Karakurt.

ACKNOWLEDGMENTS

I would probably not believe if somebody had told me that my master's degree would take 6 years but it did. I had some academic problems, which caused me to take a year-break. I persevered and came back a year later stronger thanks to Dr. Gibson, who became my academic advisor again. I would like to thank Dr. Richard Gibson for his extreme patience, encouragement, and never-ending support. I believe he is the real architect of my success because his guidance and advice made me achieve my goals here at Texas A&M University. Most importantly, I am grateful that he believed in me. He is an admirable and a friendly person and a successful academic advisor. Special thanks and appreciation go to my committee members, Dr. Joel Watkins, Dr. Steven Dorobek and Dr. Duane McVay for their understanding, contribution and support to my research and me. I am grateful to have them in my committee.

I have to acknowledge my family because they have been amazing throughout my study. My parents, brothers, sisters, and even my nieces and nephews were always there for me. They have been extremely understanding as they stood by me. I have always had their solid support no matter what it is that I am going through. I believe their prayers and love kept me going. They have never given up on me and I am glad that they did not.

Last but not least, I would like to thank my wife, Norma Karakurt. She has been quite patient even though she has suffered a lot with me. She has faced great amounts of emotional hardship caused by me. I am amazed and grateful that she always managed to stick around and not give up on me. She has supported me both emotionally and economically. I am glad to have her on my side.

Finally, I am sure I have frustrated a few people during my education. It is not common to apologize in this section but I would like to apologize to those, whom I hurt, annoyed or frustrated with all my questions, discussions and arguments. Overall, I think it has been an amazing journey to pursue an M.S. degree in geophysics at Texas A&M University even though it always felt it would never end.

TABLE OF CONTENTS

Page

CHAPTER Page

LIST OF FIGURES

FIGURE Page

FIGURE Page

FIGURE Page

CHAPTER I

INTRODUCTION

The Cut Bank oil and gas field in Montana has been subject to attention by petroleum explorers and developers since hydrocarbon production began in 1926. Different companies drilled a number of wells over the years. Recent dry wells and water flooding program raised concerns about finding the right drill locations, which eventually led the industry to redevelop the current reservoirs by gathering and recording seismic data in the area. To serve the purpose, a 3-D surface seismic survey was gathered, and a variety of well logging was also recorded in the wells. 3-D seismic survey and vertical seismic profiling (VSP) well and Cut Bank field locations are displayed in Figure 1.1. Geology of the area has been well known and the reservoirs are formed in an incised-valley system, where alluvial braided-stream type deposition occurred.

Surface seismic has proven the existence of this valley-like structure and also brought to our attention a high attenuative zone right above so-called reservoir sequence. This highly attenuative zone is called Bentonite, volcanic ash, which is approximately 20-40 ft thick throughout the area. The seismic section in Figure 1.2 shows the layer tops around the reservoir including Cut Bank sand units and the Bentonite layer. A noticeable change in the signal trend in 3-D seismic sections below this attenuative zone is apparent and raises the question of "How much does the Bentonite alter the seismic amplitudes of waves propagating through it?". The main goal of this study is to investigate the effects of this highly attenuative Bentonite layer on seismic signals. Studying the changes in the signals is vital to the study because 1) seismic analysis depend on observation of characteristics of seismic signals; and 2) signal characteristics depend on the media they propagate through. With this in mind, this study is aimed to utilize VSP data taken within the seismic survey to help with the seismic characterization of the targeted sand units and the thin Bentonite layer over the reservoir. The goal is to focus on the seismic attenuation in Bentonite and how it affects the seismic amplitudes from signals traveled within and below this

---

This thesis follows the style and format of Geophysics.

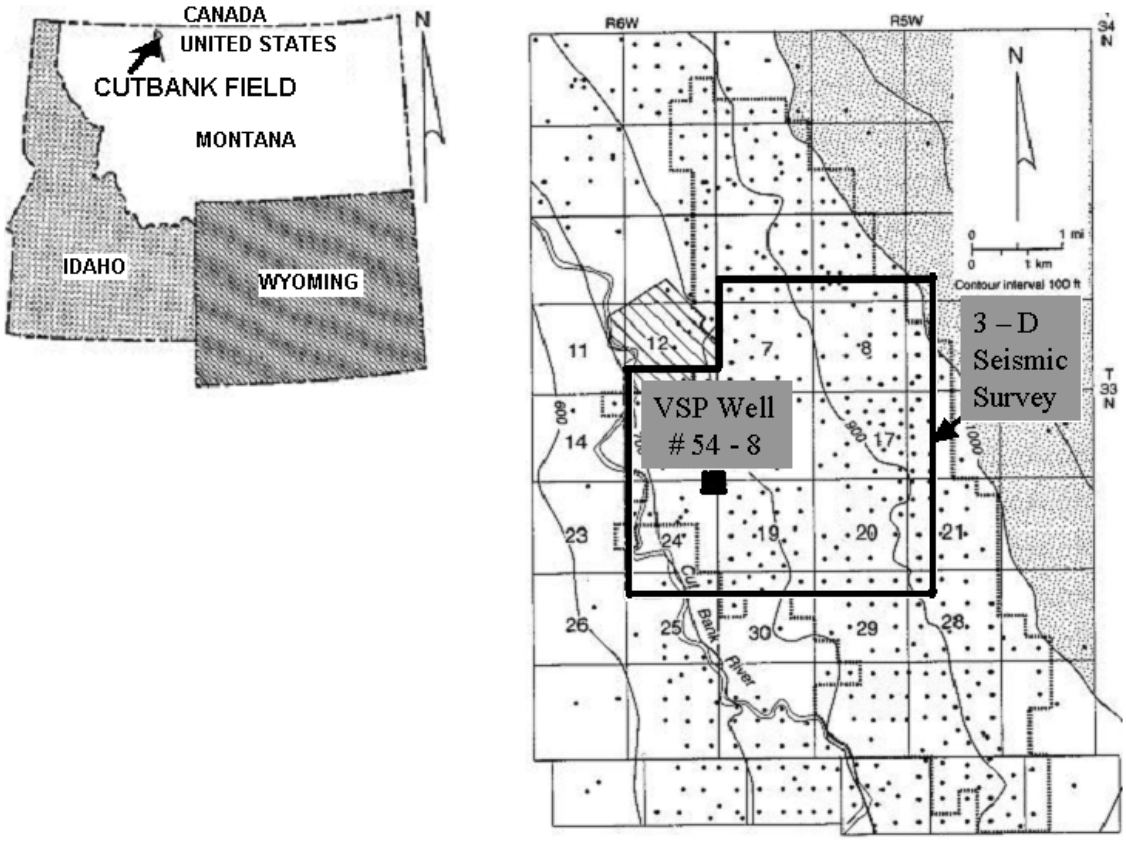

Fig. 1.1. Location of Cut Bank oil field (left), 3-D seismic survey VSP well # 54-8 (right). Adopted from (DeAngelo and Hardage, 2001).

layer. Below, I first review the geology of the area, and then briefly introduce the goals and methods of the attenuation analysis.

1.1 Geology of the Area

1.1.1 General Description

The surface rocks of the area are covered by a mantle of glacial drift Pleistocene age, that consist of soil, clay, gravel, and boulders (Romine, 1929). Exposed rocks on the surface range in age from Two Medicine of the Upper Cretaceous to the Kootenai of the Lower Cretaceous. Hydrocarbons are produced from the Kootenai formation and that is why information about this formation will be of interest. The Kootenai formation lies over Ellis formation of Jurassic age, which is a gray to dark, gray, and green calcareous shale and accepted as the base rock. Above the Kootenai formation,

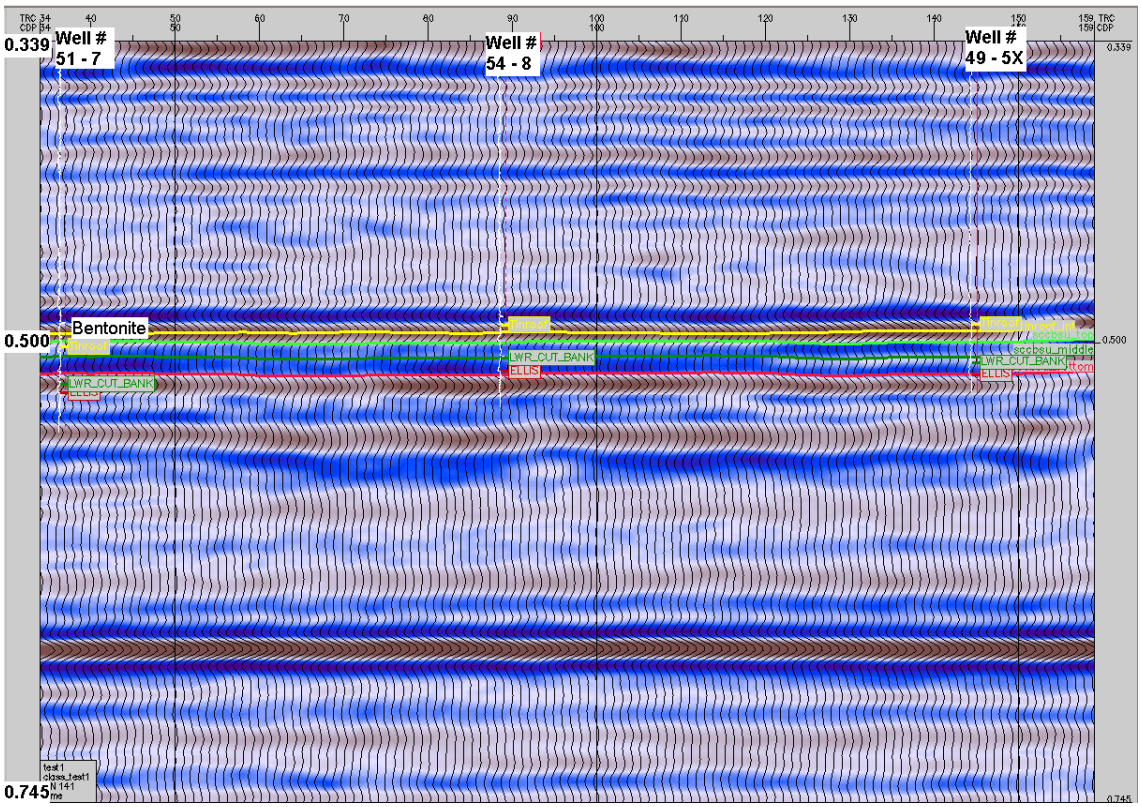

Fig. 1.2. Seismic section crossing through VSP well # 54-8 on 3-D seismic survey from south central Cut Bank unit.

there is the Colorado group, which is a thick sequence of gray to black marine shale with thin beds of calcareous concentrations and a few thin sands in the upper level of the formation. The Kootenai consists of red, green, yellow, and dark gray sandy clay shales with irregular lime and sandstone lenses. Its thickness ranges from 300 to 500 ft (Romine, 1929). The gas sands in the Kootenai group are named Moulton, Sunburst, and Cut Bank sands. See Figure 1.3. The Cut Bank sand at the base of the group is more porous and the best pay sand (Bartram and Erdman, 1933). It consists of cherty and conglomeratic facies.

1.1.2 Depositional Model

The texture and structure of the pay sandstone indicates low-energy system conditions over high-energy system depositions. The structures change upward from flat bedding to ripple laminated layers whereas the texture grades upward from conglomerate to find grain sand (Weimer and Tillman, 1980). The Cut Bank sandstone is

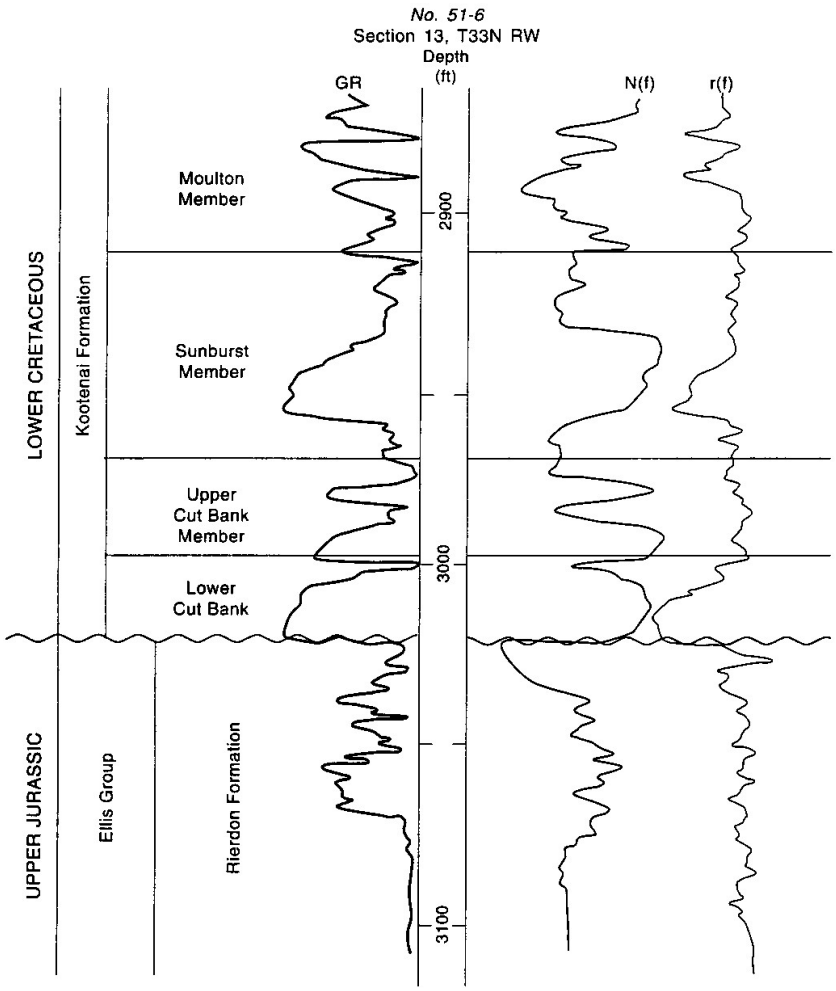

Fig. 1.3. Cut Bank oil field sand units at well # 51-6, taken from (DeAngelo and Hardage, 2001).

interpreted as point bar sandstones associated with meandering stream channel of a broad alluvial valley. The bottom seal is the impermeable marine shale (Ellis group) and the top seal is again impermeable mudstone of the flood plain environment (Colorado Shale). Oil and gas accumulation is believed to be in abandoned channel fill, which is impermeable, and the accumulation occurs in structural traps.

1.2 Previous Studies

Previous studies include only a 3-D seismic survey acquired over an 8 mi^2 section of Cut Bank field in Glacier County, Montana. See Figure 1.1. The main purpose of the

study was to optimize an ongoing waterflood program that was being implemented to sustain production at Cut Bank field (DeAngelo and Hardage, 2001). The 3-D seismic shot was made by Western Geophysical in the southeast of the city of Cut Bank, Montana, and processed and interpreted by (DeAngelo and Hardage, 2001). According to the report provided by Quick Silver Inc., (DeAngelo and Hardage, 2001) noticed the presence of channel systems after using traditional horizon-slice imaging of seismic reflection amplitudes. Then they ran a 3-D seismic coherency technique to increase the resolution of the image in the channel systems. As they explain, the 3-D Coherency method is an examination of adjacent traces in the 3-D surface seismic data. After applying the technique, they were able to define several channel systems within the survey. Two of these channels were clearly identified in the 3-D seismic time slice impedance volumes, one at the time depth of 410 to 460 ms, and the other at the time depth of 480 to 520 ms.

The well log information in the area is primarily from density, porosity and gamma-ray logging. The absence of sonic logs made well to seismic tie impossible. (Hardage, 1995) concluded that VSP data, when properly recorded and processed, is the most accurate source of information to establish the detailed depth versus time calibration required to seismically distinguish closely spaced thin beds. For this reason, (DeAngelo and Hardage, 2001) recorded VSP data in the well named SCCBSU No. 54-8 using the source offsets of 550 ft (near offset) and 1100 ft (far offset). See Figure 1.1 for the location of the well SCCBSU No. 54-8. As they stated, near offset recordings would be enough to identify thin reservoir sand units in the Cut Bank oil field. Next, the processed VSP data was tied to surface seismic to increase the image quality.

In conclusion, the presence of a low velocity Bentonite layer overlying the reservoir sands appears to absorb much of the higher frequency energy, degrading the high frequency component of the illuminating wave field below the Bentonite structure (DeAngelo and Hardage, 2001). Finally, five new well locations were identified and one of these wells encountered no reservoir sands even though it was out of the incised valley system.

1.3 Estimation of Attenuation Properties

Previous studies have not focused on the properties of Bentonite itself, which is why this research faces big challenges. However, I will analyze the VSP data and look for answers to the following questions:

- How much does Bentonite alter the seismic waves propagating through it?
- Is the effect significant or negligible?
- How do reflection characteristics vary below and above this thin layer and how can one determine the variations in reflection characteristics?
- Can one determine the seismic characteristics of Bentonite structure?
- Can attenuation analysis using VSP data be helpful to address these inquiries?

A through investigation of wave propagation and seismic signal behavior in multi-layered environment will help answer the first three questions. However, one should also remember that processing the VSP data would be helpful to understand how significant the effect is. Answering the last two questions requires a series of experimentation and tools such as choosing a suitable/reliable method for attenuation analysis.

The Spectral Ratios Method (SRM) was chosen to conduct the attenuation analysis within the VSP survey. SRM is a technique that analyzes the reduction in seismic signal amplitudes as they travel a known distance from their source, i.e. amplitude of a seismic signal becomes smaller as it travels deeper in the earth. The logarithmic ratio of seismic amplitudes at depths z_1 and z_2 provides us with the seismic information such as how attenuative the interval is.

Spectral analysis of VSP data showed high amplitude loss approximately at and below 2800 ft. Velocity profiles were extracted by commercial software. Velocity estimates for the depths 2800 and 2850 ft are 13300 and 11300 ft/s respectively. An obvious drop (2000 ft/s) in the velocity is not absolutely accurate; however, it is a sign of expected low velocity zone. Q estimations are made using SRM throughout the VSP survey. Low Q values (3 - 20) are observed within the VSP depth range; however, where Bentonite is present has the lowest Q value of approximately 5. In the remainder of this thesis, I will describe the data and the processing in more detail and then present the results of the attenuation analysis.

1.3.1 Seismic Quality Factor (Q)

Analysis of seismic wave amplitudes helps geophysicists improve the quality of seismic imaging. Each physical process affecting seismic wave amplitudes has to be considered for better analysis. One of the major factors is called attenuation, and it depends on the physical properties of rock and its fluid content. Attenuation reduces the seismic wave amplitude exponentially as it is shown in Equation 2.2. There are several different mechanisms that reduce or affect the amplitude of seismic waves and these mechanisms will be detailed in section 3 of Chapter II. As described in Equation 2.2, attenuation coefficient α represents the whole reduction in the wave amplitude. In seismic studies, attenuation coefficient is scaled by a constant as shown in Equation 2.3. The constant Q is called the quality factor, and it quantifies how much the propagating waves decay while propagating in the rock. A higher Q value corresponds to less attenuation; the lower Q is, the greater the reduction in seismic amplitude.

Lower crustal rocks are known to have higher Q values (less attenuation), likely because they have less cracks and pore fluids. Shallow crustal formations, especially sedimentary rocks, with larger grains and high pore volume tend to have lower Q values (higher attenuation). This is largely because the relative motion of fluids and solids in the rock leads to loss of energy as the wave propagates. This type of energy loss accounts for attenuation and the amount of seismic Q can help us determine the above types of physical properties of the rocks.

There have been many seismic studies aimed at determining seismic Q values for different type of rocks and materials all around the world, and many of the estimates are made through SRM using VSP data sets. Most Q estimates for shallow crustal rocks vary in the range of 10 to 100. The Bentonite layer in the Cut Bank field is a volcanic ash deposit and is of basaltic origin. Seismic Q for basaltic rocks averages between 10 and 45 (Shaw et al., 2004). The Q estimate for the Bentonite layer in the Cut Bank area might fall on this range since it is also a basaltic rock.

CHAPTER II

VERTICAL SEISMIC PROFILING

2.1 Vertical Seismic Profiling

In the conventional surface seismic studies, geophones and the source are placed along the surface on the ground. The difference with vertical seismic profiling is that in VSP studies, receivers are placed vertically along the borehole while the source is kept on the surface or in an adjacent well. Because the profile is vertical, we can observe the seismic waveform and how it evolves as it propagates through the earth. VSP has become a common tool used in seismic exploration. What separates VSP from surface seismic is that VSP measures one-way travel time as opposed to surface seismic measuring two-way travel time. VSPs, of-course, require extensive data processing as surface seismic does, and most, if not all, seismic processing techniques can be applied to VSP with little changes. Deconvolution, AVO and spectral analysis can be mentioned as a few of the seismic processing techniques. VSP can be used in parallel with the surface seismic or be assessed as a second source of interpretation in the exploration. Therefore, we can image the earth most effectively, for example, establishing well-to-seismic ties can improve the reliability of seismic interpretation.

Relations between acoustic parameters and important rock properties can be examined. Figure 2.1 displays a model sketch of VSP survey geometry and example of upgoing and downgoing wave trends. Unlike surface seismic, separation of up-going and down-going wave trends is much easier in the VSP recordings. Thus, we can successfully extract information on reflectivity, attenuation, mode conversions, velocity and other rock properties such as porosity and permeability.

2.2 Methodology

2.2.1 General Information

The source used in VSP studies can be explosives, airguns, or vibrators, however using explosives will increase the cost and can damage the source well. VSP record-

ings are either far offset or zero (near) offset depending on the type of the study. Different surveys require different processing techniques, however, general VSP processing steps involve editing, stacking, static correction, frequency and velocity filtering, wavelet shaping, amplitude analysis, deconvolution, transfer function calculation, and impedance estimation. Some of these steps can be omitted and/or some other techniques can be required for the specific data set.

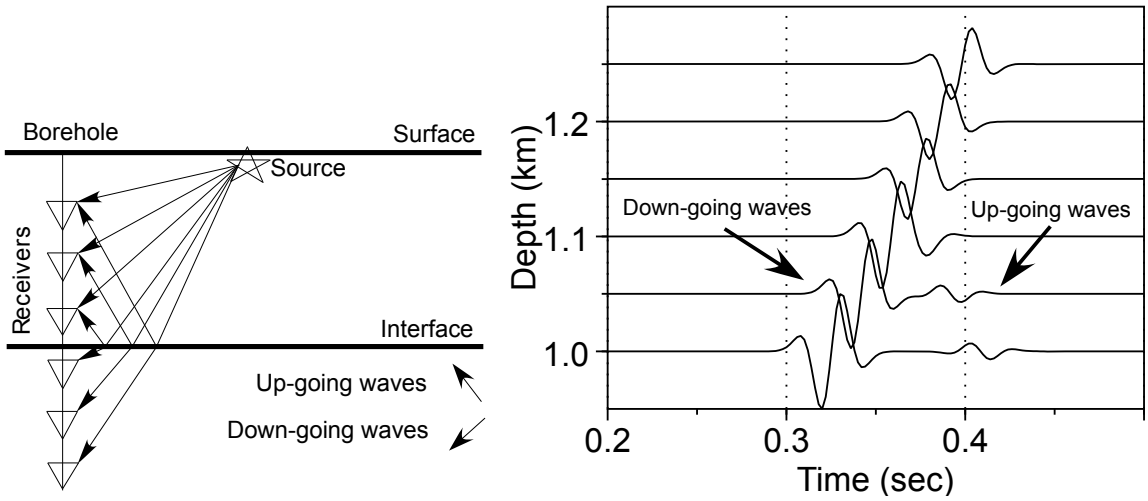

Fig. 2.1. Display of a VSP survey geometry (left) and a typical VSP recording (right).

2.2.2 Data Analysis

Analyzing the field data is important. The complexity or the simplicity of the analysis depends on what kind of seismic processes and how each process applied to the data. For example, the better one can pick first arrivals the better estimates of velocities one can get. Thus each seismic processing tool has importance to the use of field data. Processing tools and how they are applied to the VSP data is not the main goal of this study. That is why the study will only focus on the tools that will help understanding the concept of the study.

2.2.2.a Velocity Survey

Picking up first arrival time is always a challenge in seismic studies. Getting the correct arrival time of a signal always depends on the applicant because everybody has their own style and uses their own judgment. The main purpose to obtain the

correct arrival time is to be able to better estimate the velocity information. Different first break picking styles were applied to the Cutbank field data. The main idea was to determine the most reliable velocity estimates for the study area. The first break picking styles and their results along with Cutbank field VSP data processing will be discussed in Chapter III.

2.2.2.b Median Filter and VSP to Surface Seismic Tie

Median filter is a useful data processing tool that separates the up-going waves from down-going waves. This study contains uses of commercial VSP software Seislink, created and distributed by Baker Hughes, in many aspects of data processing. The software provides a variety of tools such as velocity survey and median filter. Simply separation of down-going signals (direct arrivals) from the field data yields the up-going waves (reflected events). One can tie the VSP to the 3-D Seismic reflection data. Thus one can be sure if the processing is satisfactory. Reflection characteristics in the VSP matched those in the surface seismic even though there is about 30 ms time shift due to apparent difference in the datum level. Value of datum level for surface seismic was not available for this study.

The layer boundaries from the available logs (gamma-ray and density) also were useful as a reference. Although each layer top is clearly separable from these logs, only major reflections are easy to follow on median filter applied VSP. The reflections from the thin layers are not clearly identified on either the VSP or surface seismic data. However, matching major reflections was successful even though there were small differences in the reflection characteristics and reverse polarity was observed.

2.3 Attenuation

Attenuation is the decay in the amplitudes of the seismic waves propagating through the earth. There are two types of attenuation, intrinsic and non-intrinsic attenuation. Non-intrinsic (apparent) attenuation can occur naturally because scattering of waves from irregularities inside the earth. This alters seismic waveforms in much the same way as does true attenuation that is associated with amplitude decay. Seismic characteristics such as velocity and density of the medium also cause attenuation that we aim to measure. Intrinsic attenuation is a result of fluid-to-rock and rock-to-rock

interactions of the earth when seismic signals pass through them. This type of attenuation is highly dependent of the fluid type and its content. There is no clear or obvious information about this type of attenuation and studies have been conducted on the subject.

In contrast with attenuation, geometrical spreading is a result of spherical spreading behavior of the seismic waves. The wave energy is distributed along the surface of the sphere, which enlarges as the travel distance increases. As a result, wave energy becomes smaller in time or as we get farther from the source. In other words, geometrical spreading loss could be recovered with consideration of the distance a seismic wave travels. Scattering occurs at irregular boundaries such as fault-line and structure that vanish or start in the earth. Scattering effects depend upon the geometry of the irregularity. Multiples are resulted from the layering effect. They have fundamental importance in the transmission of the seismic wave energy since they affect the signals in a constructive way. Thus not only do multiples carry energy downward but they also produce a broadening of the downgoing wavelet, which is similar to that caused by intrinsic attenuation. As is well known, when a seismic wave hits an interface, some of its energy is reflected and some of it is transmitted to the medium below, and some of it will convert to different wave modes such as a p-wave creating an s-wave. Mode conversion also results in amplitude decrease of the wave energy. All the effects mentioned above need to be accounted for a successful attenuation measurement. Attenuation caused by the physical properties of rock itself is the focus of this study and is named just "the attenuation". The attenuation is directly related to the rock properties and it is unique to the rock itself. So finding the attenuation for each specific rock helps us characterize each individual rock and their parameters, and gives us some ideas about their seismic behavior.

Attenuation analysis of the elastic waves has been widely used in seismic studies. The intent is not to go into details of the attenuation measurements; however, brief information about what has been done regarding attenuation measurements for VSP studies could be useful to the reader. Elastic absorption in rocks is a highly variable parameter, which depends on confining pressure, porosity, degree of fluid saturation, and fluid type as demonstrated in the laboratory (Toksoz et al., 1979),(Winkler and Nur, 1979), (Johnston and Toksoz, 1980). The major attenuation mechanisms presently known include matrix anelasticity which involves frictional dissipation resulting from relative motion of solid boundaries and across surfaces of cracks (Walsh,

1966), fluid flow with relaxation due to shear motions at pore fluid boundaries (Walsh, 1969), (Solomon, 1973), dissipation in a fully saturated rock as a result of the relative motion of the solid frame with respect to fluid inclusions (Biot, 1956a; Biot, 1956b), (Stoll and Bryan, 1970), squirting an enhanced intra-crack flow phenomena (Mavko and Nur, 1975), (Mavko and Nur, 1979), and geometrical effects including scattering off grains and pores (Kuster and Toksoz, 1974). The factors that cause attenuation and reduction in the velocity of seismic waves propagating through earth materials are also known to control porosity and permeability (Klimentos and McCann, 1990). Seismic source generates different amount of stress and tension when it is not coupled on the ground because of relocation or increased oil compaction after each shot. A buried monitor geophone near the source should be used to record the signals and to correct the VSP traces (Balch et al., 1982).

2.3.1 Seismic Amplitude and Attenuation

Seismic amplitude is the amount of energy carried within a seismic signal. The basic definition of seismic amplitude of a plane wave traveling in a homogenous medium as a function of time can be written as follows:

$$a(t) = a_0 + e^{i(wt - kz)} \tag{2.1}$$

where a_0 is the initial energy of the propagating wave (energy at source), $a(t)$ is the wave energy after distance z. w and t are the radial frequency and time respectively. The Equation 2.1 is the simplest form of the seismic energy, as it is not affected by any factors during propagation of the wave. It assumes that the seismic wave propagates in a homogenous medium i.e. there is no energy loss. As we know seismic waves lose their energy content as they travel in the earth. Indeed, each factor that causes energy loss in the seismic wave must be added to the Equation 2.1 so it can fully represent the energy of a seismic wave. Lets rewrite Equation 2.1:

$$a(t) \;=\; a_0(t) * s(t) * r(t) * g(t) * tr(t) * e^{-(\alpha z)} e^{i(wt - kz)}, \tag{2.2}$$

where the $*$ symbol indicates convolution. Equation 2.2 includes all known possible factors effecting the amplitude such as $s(t)$ and $r(t)$ source and geophone coupling, $g(t)$ geometrical spreading, $tr(t)$ reflection and/or transmission loss effects. The second exponential term $e^{-\alpha z}$represents attenuation. The most common measure of seismic

attenuation is dimensionless quality factor (Q) or its inverse ($\frac{1}{Q}$). Q relates the attenuation as:

$$\frac{1}{Q} = \frac{\alpha V}{\pi f \; - \; \frac{\alpha^2 V^2}{4\pi f}} \tag{2.3}$$

where f is the frequency of the propagating wave, and V is the velocity of the medium. The term $\frac{\alpha^2 V^2}{4\pi f}$ is mainly used in scattering attenuation measurements and usually dropped under the low loss assumption. Equation 2.3 shows that seismic Q is the loss of energy in one cycle of time. Therefore, small changes in the wave energy may result in very large difference in the quality factor (Q). Furthermore, seismic wave attenuation depends on the velocity of the medium (V) and the frequency content of the elastic wave (f). Since $V = z/t$, the distance z and the seismic travel time t are also factors that affect seismic wave attenuation. However, this study will focus on the attenuation-frequency relation to investigate the seismic characteristics of Bentonite layer under the assumption that velocity of a layer is constant within the layer or the concerned depth interval.

2.3.2 Spectral Ratios Method

There are different techniques to measure attenuation from seismic recordings. Major well-known methods are amplitude decay, pulse broadening and spectral ratios. Amplitude decay measures how much seismic amplitude of the first event decayed with distance. Amplitude is corrected for the geometrical spreading loss and remaining amplitude decay counted as attenuation. Pulse broadening focuses on the changes in the width of the seismic pulse with distance. This type of measurements can give reliable results in the saturated rocks. The most commonly used method is the spectral ratios method (SRM). SRM is based on the assumption that the ratio of seismic amplitudes at two different depths is a linear function of frequency. Having a VSP data in hand, where the receivers located downwards in the borehole, SRM suits the purpose of the study of Bentonite layer in the Cutbank oil field.

Equation 2.2 has to be reconfigured to fit the requirements of SRM since seismic energy is a function of time and seismic amplitude is a function of frequency. At this point, seismic energy in time domain has to be converted to seismic amplitude in frequency domain. To be able to achieve this, Fast Fourier Transform (FFT) is applied to the data. As a result, reconstruction of Equation 2.2 as a function of frequency is required. Equation 2.2 can be rewritten in the frequency domain since

multiplication replaces sum in the FFT process:

$$A(w) \;=\; A_0(w)S(w)R(w)G(w)TR(w)e^{-(\alpha\, z)}e^{i(wt\,-\,kz)} \tag{2.4}$$

All the parameters in Equation 2.4 are the same as the ones in Equation 2.2 except they are now function of frequency. The Equation 2.4 is a generalized form of seismic amplitude since it includes all the possible effects that cause energy loss. $S(w)$ and $R(w)$ can be omitted if the data is corrected for the source and receiver coupling. The geometrical spreading $G(w)$ is a function of distance and transmission and reflection losses $TR(w)$ are a function of incident angle and velocity so they are not a function of frequency and can be treated as constant values. Now we can rewrite Equation 2.4 with these in mind:

$$A(w) \;=\; A_0(w)G\;\; TRe^{-(\alpha\, z)}\;\; e^{i(wt\,-\,kz)} \tag{2.5}$$

At this stage, the propagation term $e^{-(\alpha\, z)}$ can be rewritten to fit our purpose as follows:

$$\alpha \;=\; \gamma\, f \;=\; \frac{\pi\, f}{Q\, V} \tag{2.6}$$

Combining the parameters G and TR into GT, now we can rewrite the Equation 2.5 as:

$$A(f) \;=\; A_0(f)GT\;\; e^{-(\gamma\, z)f} \tag{2.7}$$

If we combine the amplitude terms on one side, we obtain Equation 2.8 as:

$$\frac{A(f)}{A_0(f)} \;=\; GT\; e^{-(\gamma\, z)f} \tag{2.8}$$

Now taking the logarithms of both sides of Equation 2.8, we get the explanation of SRM itself:

$$ln|\frac{A(f)}{A_0(f)}| \;=\; lnGT \;-\; (\gamma\, z)f \tag{2.9}$$

The Equation 2.9 states that logarithmic ratios of amplitudes at a distance from each other is a linear function of frequency since the simple form of Equation 2.9 can be written in the form:

$$y \;=\; a \;+\; b\, f \tag{2.10}$$

Plotting logarithmic ratios against frequency will give a linear trend, and the slope of the amplitude ratio measurements will give the b values since a is a single constant

value. If the slope of this linear trend can be calculated, the seismic Q can be calculated, because the slope equals to $\gamma\, z$ and γ relates to Q as defined in Equation 2.6.

2.3.2.a Attenuation Effects on Seismic Signals

As previously stated in Chapter II and III, attenuation alters seismic signal energy. The change in seismic energy depends upon the amount of attenuation. The higher the attenuation is the larger the reduction in the seismic amplitude. When seismic signals are attenuated, they tend to stretch in time. Signal stretching means larger wavelength, which produces smaller wave number in frequency domain. Narrower wave number is a result of amplitude loss at each frequency in the spectrum. Since the amplitude at higher frequencies has smaller values they diminish and become nearly zero. Figure 2.2 displays time signal with (blue) and without (orange) attenuation and the corresponding amplitude spectra. The spectrum looks like it has energy in a smaller frequency range and the highest (peak) amplitude is shifted by attenuation.

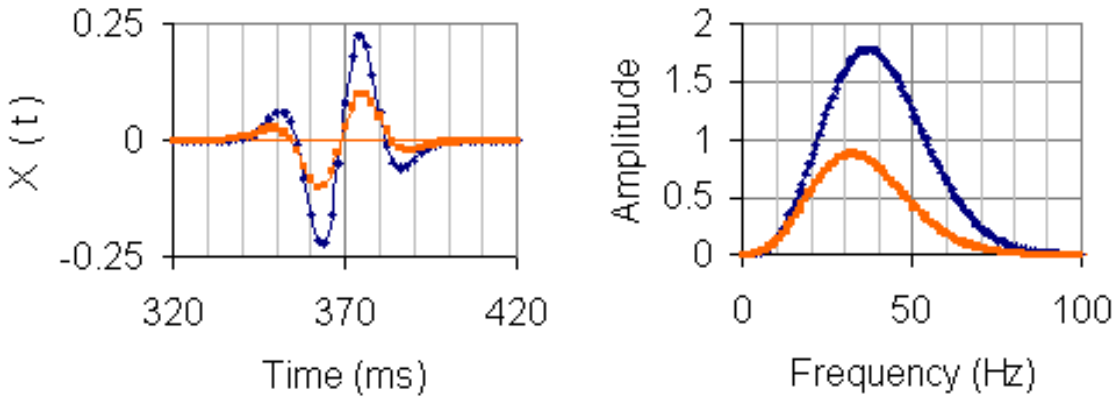

Fig. 2.2. Effects of attenuation on seismic signals (left) and their amplitudes (right).

CHAPTER III

SYNTHETIC SEISMOGRAMS

3.1 Synthetic Seismograms

Seismograms can be synthesized by evaluating the wave equation numerically. Of course, the computed (synthetic) seismograms do not include each and every effect that the earth might produce. However, we can design synthetic seismograms to satisfy the need for the seismic studies such as understanding seismic wave behavior in a half space model with and without attenuation. Once we compute synthetics we can analyze them and understand how, for instance, the attenuation alters the seismic signals. Expectations from synthetics can be thought as providing us with the information of how certain earth models respond to the distribution of seismic waves and what kind of changes in the signal characteristics are observed.

The main purpose of using synthetic seismograms in this study is to test if the SRM works well and is a reliable method to proceed with the attenuation measurements. The model to test the SRM is chosen, at first, a simple isotropic half space model. Later the model was adjusted to have some complexity such as having two layers and different attenuation mechanisms.

3.2 Isotropic Half Space Model Synthetics

An isotropic half space is the simplest model that there could possibly be even though such media does not exist in the earth. Using a model as simple as there could be is always a good idea not only to understand the seismic waveforms but also to analyze the propagation of the seismic waves. The model will not produce any reflected events since it is a single homogenous solid layer. The synthetics are computed twice for the same model having attenuation and not having attenuation. In either case, synthetics were computed using information for a typical shale, velocities being $V_P = 3\ km/s, V_S = 1.5\ km/s$ and density being $\rho = 2.5\ g/cm^3$. Receivers are placed starting at 1 km with 100 m spacing. The source was located at the surface.

3.2.1 Non-attenuative Model

The first attempt is for the model without attenuation. According to the definition of SRM, ratio vs. frequency plot will have to be a line. Since there is no attenuation in the model, the linear line has to be flat i.e. the slope has to be zero since $Q = \infty$. Figure 3.1 displays time signals, the amplitude spectra for the isotropic half space model and the logarithmic ratio plot between the two spectra. Note that the decay in the seismic energy and the amplitude is due to geometrical spreading effect. Ratio plot is not completely a flat line but in certain frequency interval from 10 to 70 Hz it significantly is a flat line, which proves that the theory of SRM is correct. We still need to fit a line to the ratio curve and calculate the slope of the fitted line so that we can estimate Q using linearity function of SRM.

The line fit to the ratio values shown in Figure 3.1 is within the frequency range (10-70 Hz). The slope of fitted line is about 0.00006. The estimated Q from this slope by plugging everything in Equations 2.9 and 2.6 is about 1745. SRM estimated Q is not close to infinite but it is noticeably high. One important observation is that the ratio curve exhibits flat line within the frequency range.

3.2.2 Attenuative Model

The above procedure was repeated for the same isotropic model with attenuation and seismic Q was chosen as 5 to represent high attenuative and 100 for low attenuative media. Figure 3.2 shows seismic signals, the amplitude spectra from the depths 1 and 1.1 km, and ratio plots of these two for $Q = 5$. Figure 3.3 shows those for $Q = 100$. In the high attenuation case, we can clearly see in Figure 3.2 that the highest (+) seismic signal energy dropped to 0.001 from 0.002 in the Figure 3.1. We can also note that seismic signals are now broadened in time as the period of the signals became larger. Amplitude spectra in Figure 3.2 show a relatively narrow frequency band of up to 50 Hz, which explains that the high frequencies are more vulnerable to attenuation than the low frequencies. The value of the estimated Q from SRM is 4.96, which has 1 % error. Estimation of Q from SRM for high attenuative medium is quite successful. Now, we need to find out if SRM will work for low attenuative medium as well. Estimated Q from this set was 103.7 with the error of 4 %. The second set of synthetics with $Q = 100$ resulted with success, too but the error amount was a little higher comparing to that of $Q = 5$.

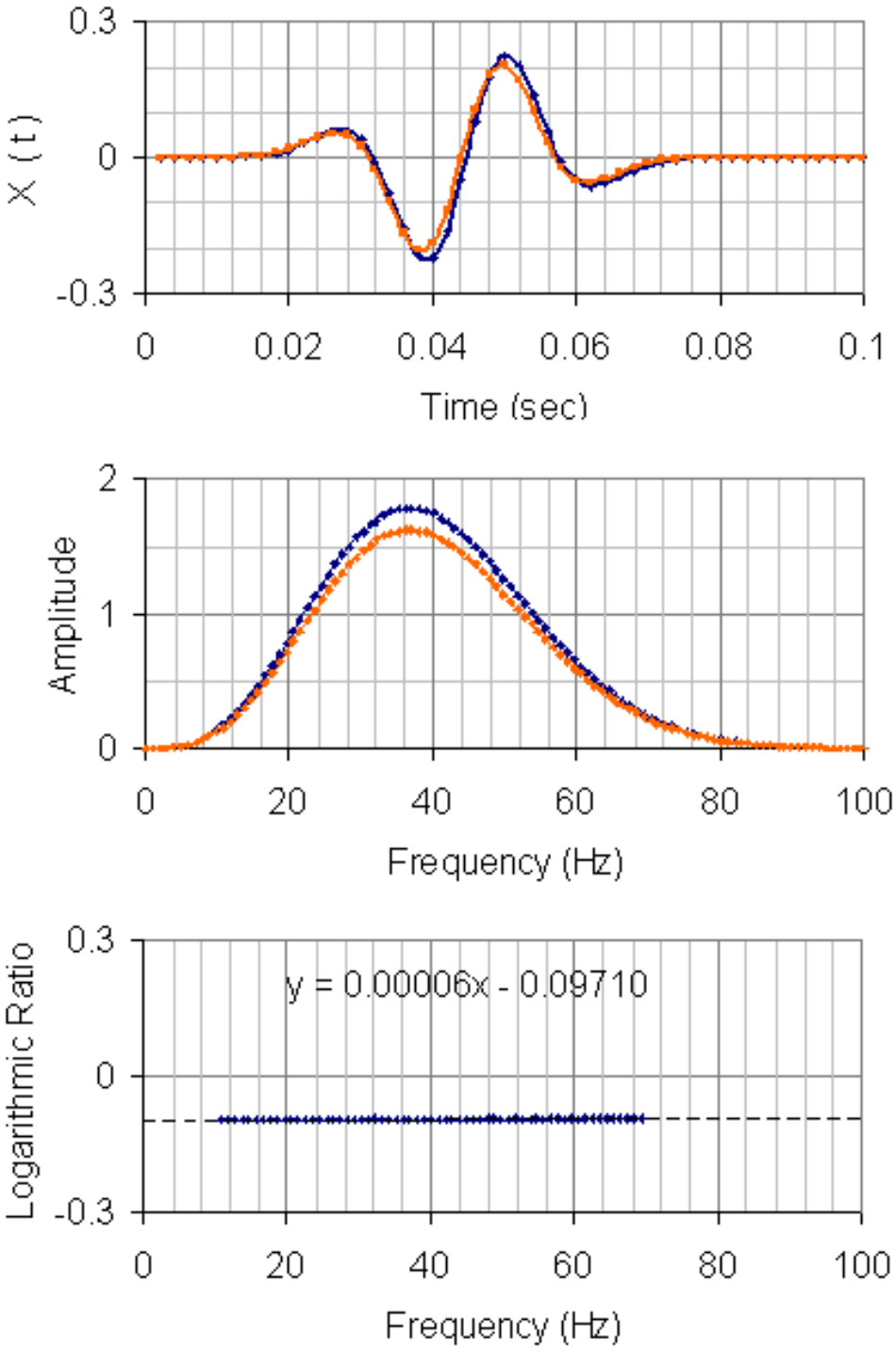

Fig. 3.1. Time signals (top), amplitude spectra (middle) and logarithmic ratio (bottom) plots for the isotropic half space model without attenuation. Blue curve in the amplitude spectra represents the amplitude spectrum of the signal recorded at 1 km and the orange curve represents that of the signal recorded at 1.05 km.

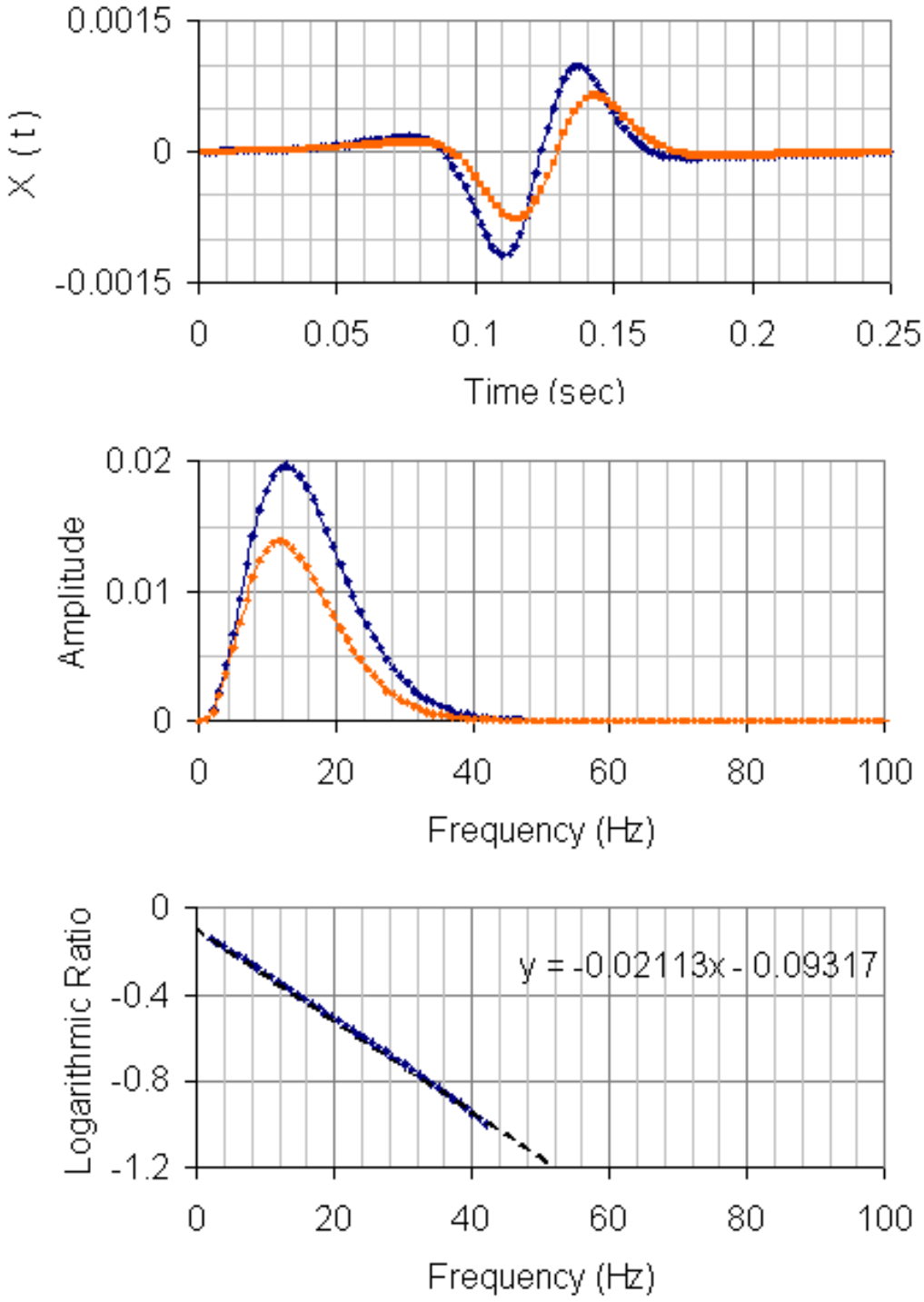

Fig. 3.2. Time signals (top), amplitude spectra (middle) and logarithmic (bottom) ratio plots for the isotropic half space model with high attenuation ($Q = 5$). Blue curve in the amplitude spectra represents the amplitude spectrum of the signal recorded at 1 km and the orange curve represents that of the signal recorded at 1.05 km.

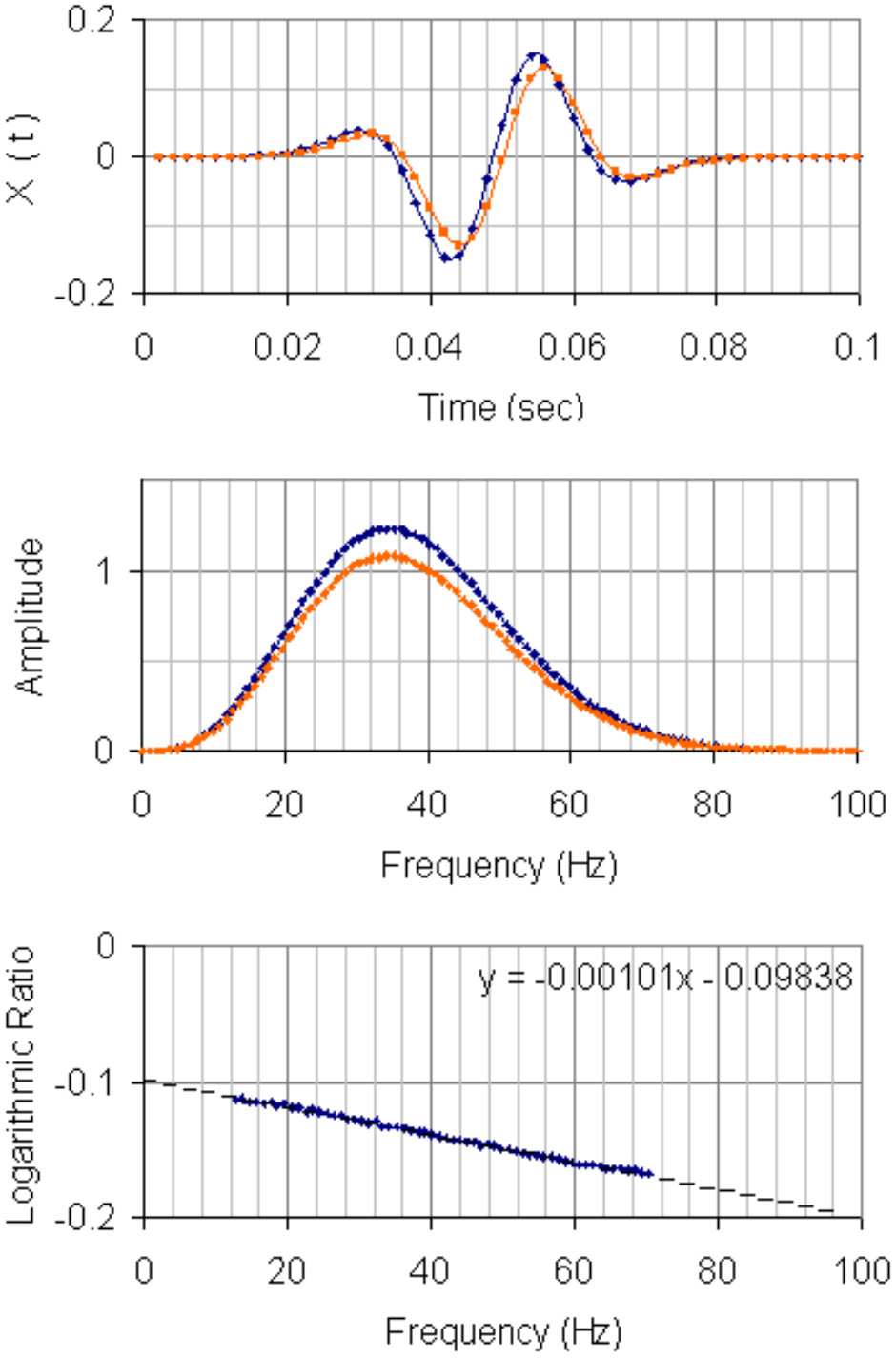

Fig. 3.3. Time signals (top), amplitude spectra (middle) and logarithmic (bottom) ratio plots for the isotropic half space model with low attenuation ($Q = 100$). Blue curve in the amplitude spectra represents the amplitude spectrum of the signal recorded at 1 km and the orange curve represents that of the signal recorded at 1.05 km.

The tests conducted using high and low attenuative media state that SRM is a good tool to estimate Q from the seismic signals. Error amounts are negligible even though the error amount is higher for the low attenuative media. The isotropic model used here is a very simple model and it proved that the SRM is a reliable technique to measure seismic attenuation. However, the question still remains as does SRM give reliable estimates for the complex geophysical models. As a result, SRM needs to be tested with the complex models. Complexity of the models comes with multi-layering and noise presence in the model. Multi-layering adds transmission and reflection losses to the data and noise could be a product of any kind of source other than the seismic source used to record the VSP survey. The accuracy of SRM must be tested against reflection-transmission and noise effects as well.

3.3 Isotropic Two Layer Model Synthetics

The second step in analyzing SRM with model synthetics is to compute seismograms for an isotropic two-layer model. We can do this by adding a layer boundary to the previously created half space model and define physical properties of a second medium. I placed the boundary at 1100 m and put two receivers on each side of the boundary with 50 m spacing. The source is again at the surface. I defined the second medium as faster than the first one, velocities being $V_P = 4\ km/s$, $V_S = 2\ km/s$ and density being $\rho = 2.7\ g/cm^3$.

Adding another layer to the model introduces reflection-transmission effects. Some of the seismic energy reflects at the boundary and some of it is transmitted to the bottom layer. There is also another factor that reduces the amount of seismic energy, which is caused by mode conversions. An explosive source itself does not create shear waves but some of the p-wave energy is converted to s-wave and reflected or transmitted at the boundaries. This study will not cover the mode conversion since it is not directly involved in the attenuation measurements. Figure 3.4 has the signals, amplitudes and the ratio plots for the first two receiver of the two-layer model. The signals also carry reflected events. Reflected energy is not as strong as the direct arrival energy but adds content to the spectrum. Amplitude spectra in Figure 3.4 has irregular harmonics in contrast to smooth curves in the one layer model (Figure 3.1). The harmonics changes the trend in the logarithmic ratio plot but the slope of the fitted line is again very small. Estimated Q is 1309 but yet not infinite as it was

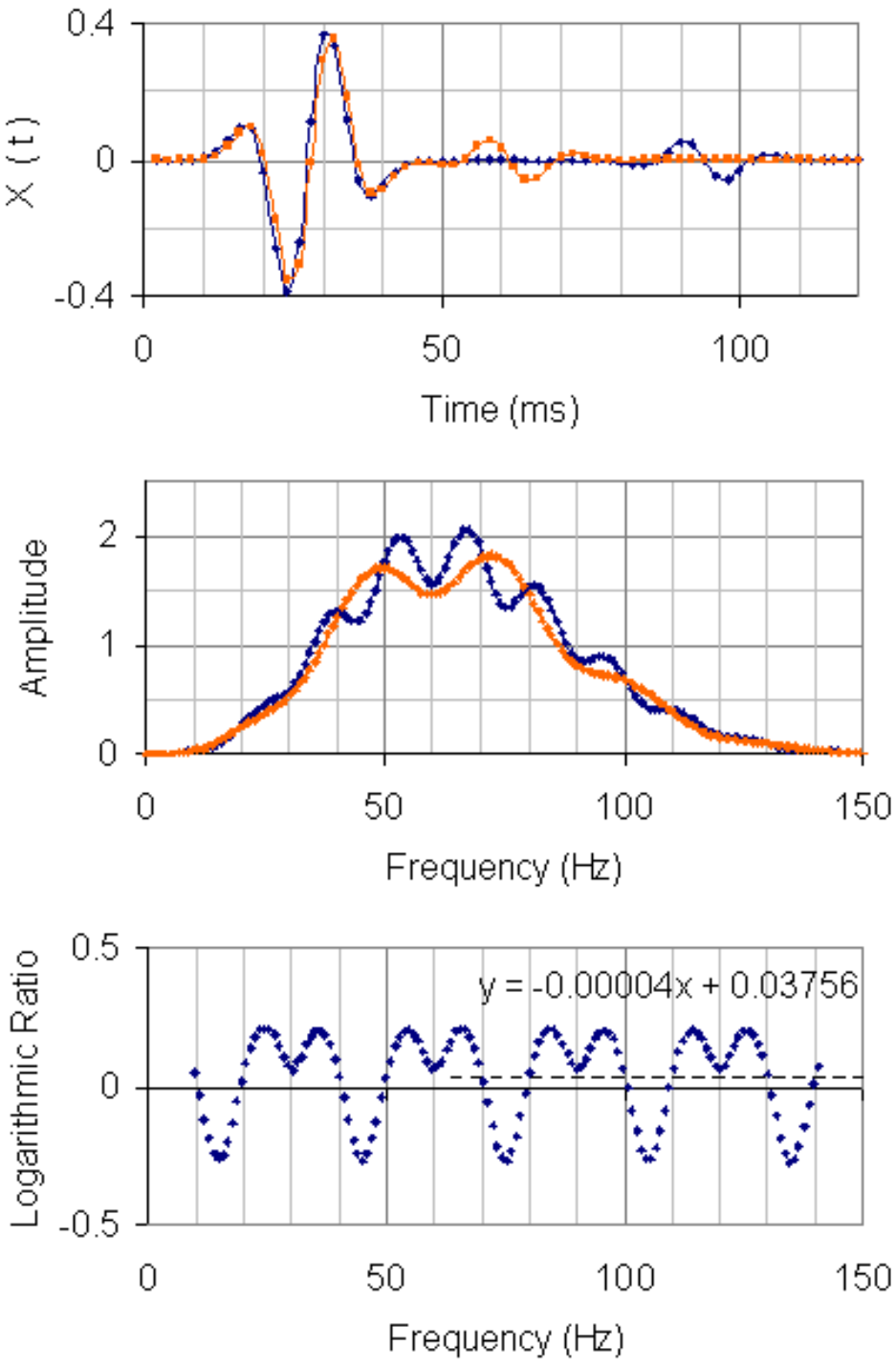

Fig. 3.4. Time signals (top), amplitude spectra (middle) and logarithmic (bottom) ratio plots for the isotropic two layer model without attenuation. Blue curve in the amplitude spectra represents the amplitude spectrum of the signal recorded at 1 km and the orange curve represents that of the signal recorded at 1.05 km.

in the one layer model. In conclusion, reflected events and mode conversions alter the seismic waveform and the amplitude; however, they do not completely change the linear trend in the spectral ratio.

3.4 Noise Analysis

It is well known that all seismic recordings somewhat have noise interference either from natural or manmade sources. Processing noisy data is not an easy task especially when the signal to noise ratio (S/N) is low. If the S/N is too low then, separation of waveforms will be very difficult or maybe even impossible. High noise amount also reduces the chances of identifying the direct arrivals, causing bad data processing and yielding wrong interpretation. The challenge is to determine how noise alters the seismic signals and how can they be eliminated and how SRM reacts to noisy data. To begin answering those concerns, the next step is to add noise to the current synthetics.

3.4.1 High Noise Interference

It is okay to start with the two-layer model since the effects of reflected and transmitted events have been analyzed in the previous sections. In this section, SRM will be tested by an isotropic two-layer model without attenuation but having $S/N = 5$. Figure 3.5 represents the model with $S/N = 5$, which has high noise presence. The seismic data presented on the Figure 3.5 are not processed to eliminate noise because we need to analyze the impact of noise interference to the seismic signals. High noise makes it very difficult to read the first arrivals in the time series, which is vital to determine the velocity information. It also covers the whole amplitude spectrum, leaving us no clue what kind of information the signals have. Overall, it is not possible to process this type of seismic data but the same time sampling and frequency sampling applied to this noisy data to see how accurately SRM will estimate the seismic Q. The Q result from SRM is 23.4 for this data set. Estimated Q is very far from infinite and represents moderately high attenuative medium.

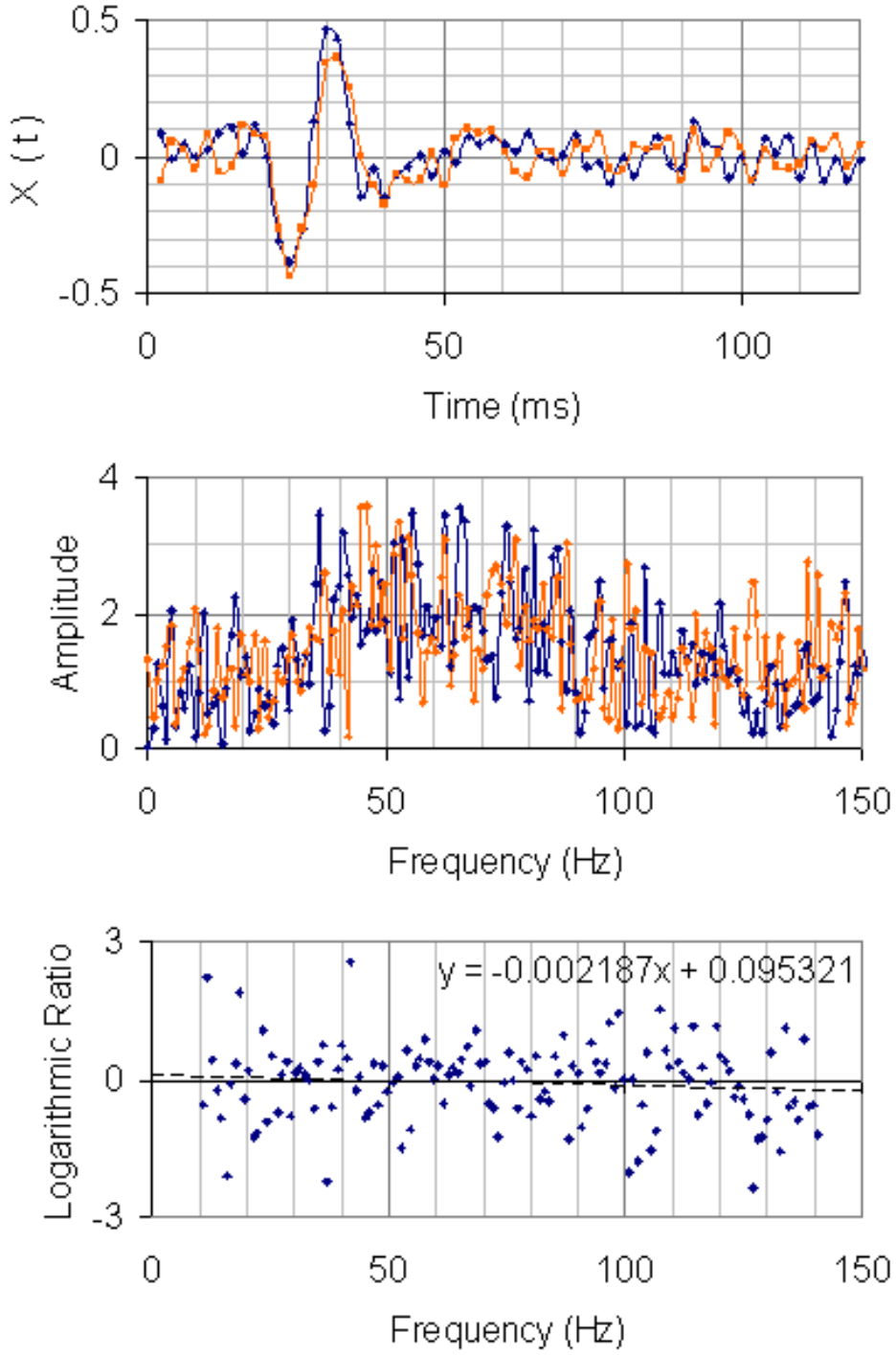

Fig. 3.5. Time signals (top), amplitude spectra (middle) and logarithmic (bottom) ratio plots for the isotropic two layer model without attenuation. High noise content added to the synthetics ($S/N = 5$). Blue curve in the amplitude spectra represents the amplitude spectrum of the signal recorded at 1 km and the orange curve represents that of the signal recorded at 1.05 km.

3.4.2 Low Noise Interference

The same two-layer model was used in this experiment but this time adding less noise ($S/N = 20$). In the previous section, high noise content almost covered the direct arrivals and made it very difficult to process the data and even estimate the seismic Q. Figure 3.6 displays the results for $S/N = 20$, which has considerably low noise presence. The data presented on the Figure 3.6 are not processed for noise elimination for the same purpose. Low noise makes it possible to recognize the reflected events. Note that high noise content was blocking the visibility of the same reflected events so the lower the noise amount is the better we can utilize and analyze the seismic data. Reading the first arrivals is a little more convenient, too. Even though noise effects are quite visible in the amplitude spectra, it is still possible to distinguish the direct arrival energy. Estimating Q from this type of seismic data is again not easy but the same time and frequency sampling applied to the data for experimentation purposes. The Q result from SRM is 74.8 for this noise level and it is again very far from infinite. However, estimation is three times more successful than estimated Q for low S/N.

In conclusion, noise makes the data processing very hard, blocks the reflected events or signals with smaller energy, greatly reduces the accuracy of Q estimation and must be eliminated from the seismic data. There are ways to eliminate the noise from the seismic data although it is not possible to completely erase the noise content. In practice, filters are applied to the seismic data either in time or frequency domain depending on the type of the filter used.

3.5 Filtering and Tapering

3.5.1 Bandpass Filter and Taper

The most common filters are bandpass filters, which eliminates the so-called noise frequency content from the data. Simply, filtering is multiplying the wanted part of the data with 1 (passing band) and multiplying the unwanted parts with 0 (filtering band). For instance, bandpass filter presented in Figure 3.7 (top) is designed to pass the data that fall on to the frequency interval from 10 to 70 Hz and to filter the rest. In practice, filters are not exactly designed like the bandpass filter in Figure 3.7 (top) because clipping the data at some frequency range will introduce harmonics, namely

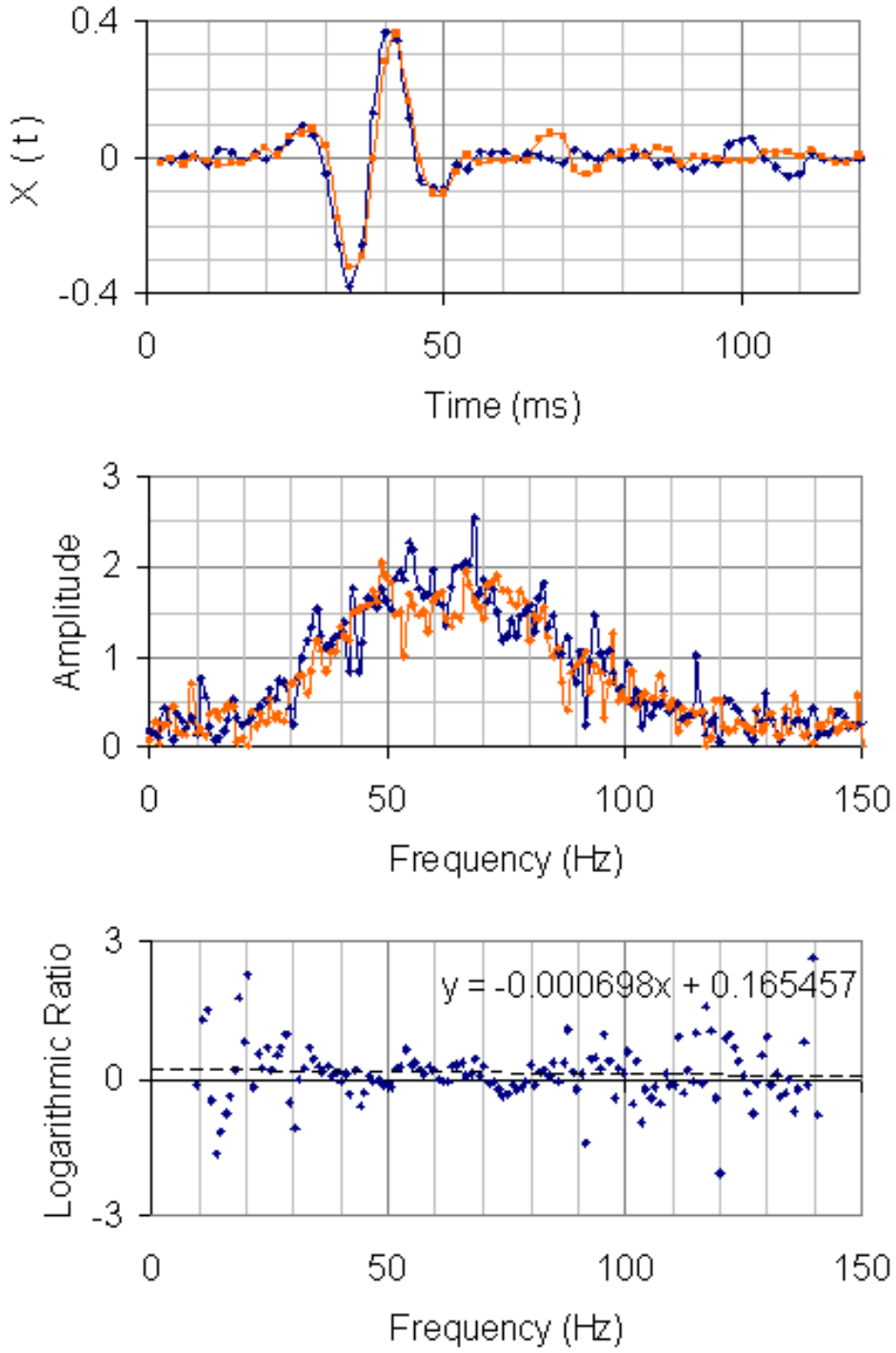

Fig. 3.6. Time signals (top), amplitude spectra (middle) and logarithmic (bottom) ratio plots for the isotropic two layer model without attenuation. Low noise content added to the synthetics ($S/N = 20$). Blue curve in the amplitude spectra represents the amplitude spectrum of the signal recorded at 1 km and the orange curve represents that of the signal recorded at 1.05 km.

noise, to the remaining portion of the data, which is an effect that we want to avoid. To overcome this problem, we need to smooth the filter's edges as displayed on Figure 3.7 (bottom). Smoothing is called tapering in seismic studies. As we can see, the filter gradually tapers information from 0 to 10 and from 70 to 100 Hz. It is obvious that not everything that falls into these intervals is filtered but the information closer to 0 and 100 Hz are filtered more.

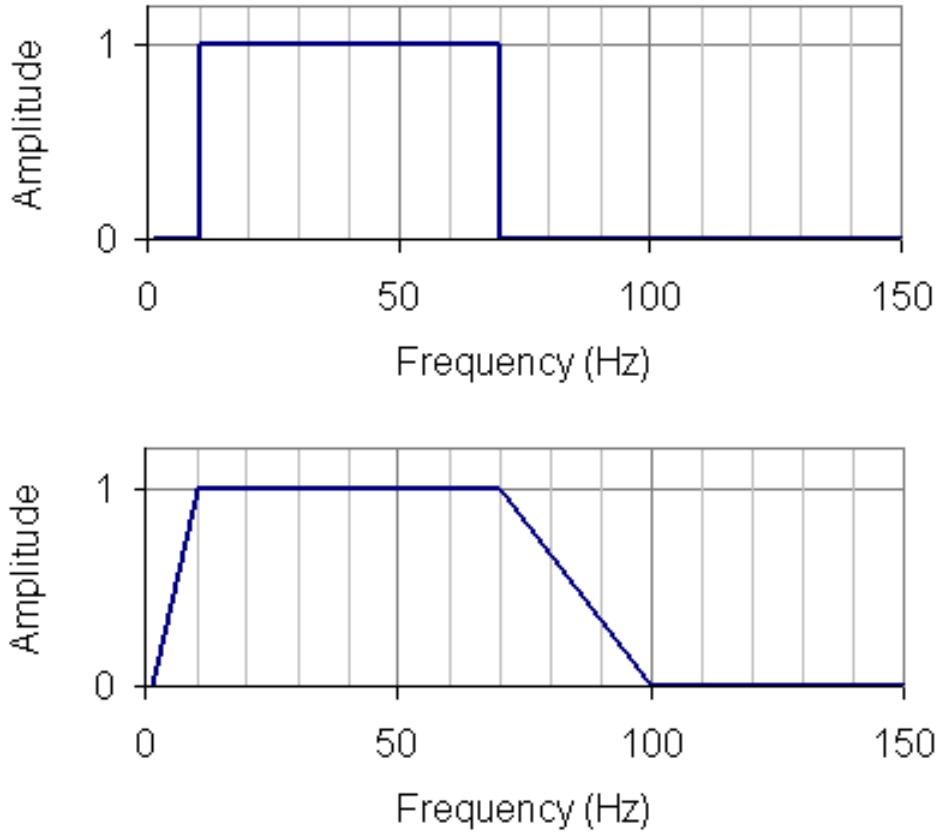

Fig. 3.7. Display of bandpass filter in with and without taper in frequency domain.

3.5.2 Median Filter

A brief description of median filter is given in Chapter I. Examples of median filter applications will be given in this section. As we know the purpose of median filter is to separate the downgoing waves from upgoing waves or vice versa. Since the earth is always multi-layered, seismic response of it always has reflected and converted events.

Median filter can eliminated these events from the seismograms. Use of Seislink for the data processing was mentioned in Chapter II. One of the Seislink utilities is the median filter tool that provides built in band pass filter. The noise can be eliminated and reflections can be separated from the downgoing waves in one step by using this Seislink utility. It is important to test how successful the median filter is. Noise added synthetics for two-layer model were used to test the median filter. Results for the $S/N = 5$ and 20 are displayed in Figure 3.8 and Figure 3.9 respectively. Time signals for each noise level show significant improvement after the application of median filter. The reflected events and noise content seem to be eliminated from the data. We can clearly propose that the median filter improves the quality of seismic signals and their amplitudes although there seems to be reduction in the seismic amplitude after median filter application. The amplitude reduction is due to filtered noise and reflected events. Estimation of Q for the data with $S/N = 5$ is 52360 and that for the $S/N = 20$ is 17455. These numbers may not be infinite but are satisfying the very low attenuation case and the success of Q estimation from SRM using median filtered data. Now that we have the tool to help us remove the noise content and also subtract the reflected events from direct arrivals, we can move on to the field data and process it accordingly with knowledge of the above experiments.

3.6 Three Layer Model Synthetics

A three layer model was also created to test the effects of a thin and highly attenuative medium on seismograms and SRM results. The model was created to imitate the Bentonite layer in the Cut Bank field so the parameters for the layers were kept as close as possible to those obtained from the VSP data set and the well-logs. Four receivers were placed with 50 ft spacing starting at 2750 ft. The thin layer was placed between the depths 2810 and 2830 ft allowing us to observe how Q estimation from SRM will react to a setting where there are three different layers between the two receivers. Velocity and density information for the layers are as follows: (Layer 1) $V_{P_1} = 14500\ ft/s$, $V_{S_1} = 8500\ ft/s$ and $\rho_1 = 2.7\ g/cm^3$; (Layer 2) $V_{P_2} = 8000\ ft/s$, $V_{S_2} = 4700\ ft/s$ and $\rho_2 = 1.7\ g/cm^3$; (Layer 3) $V_{P_3} = 12500\ ft/s$, $V_{S_3} = 7500\ ft/s$ and $\rho_3 = 2.5\ g/cm^3$. As we learned from the previous models, multiple layers produce reflected, transmitted and converted waves. However, the presence of a thin layer also results in strong multiples caused by seismic signals being trapped within the layer

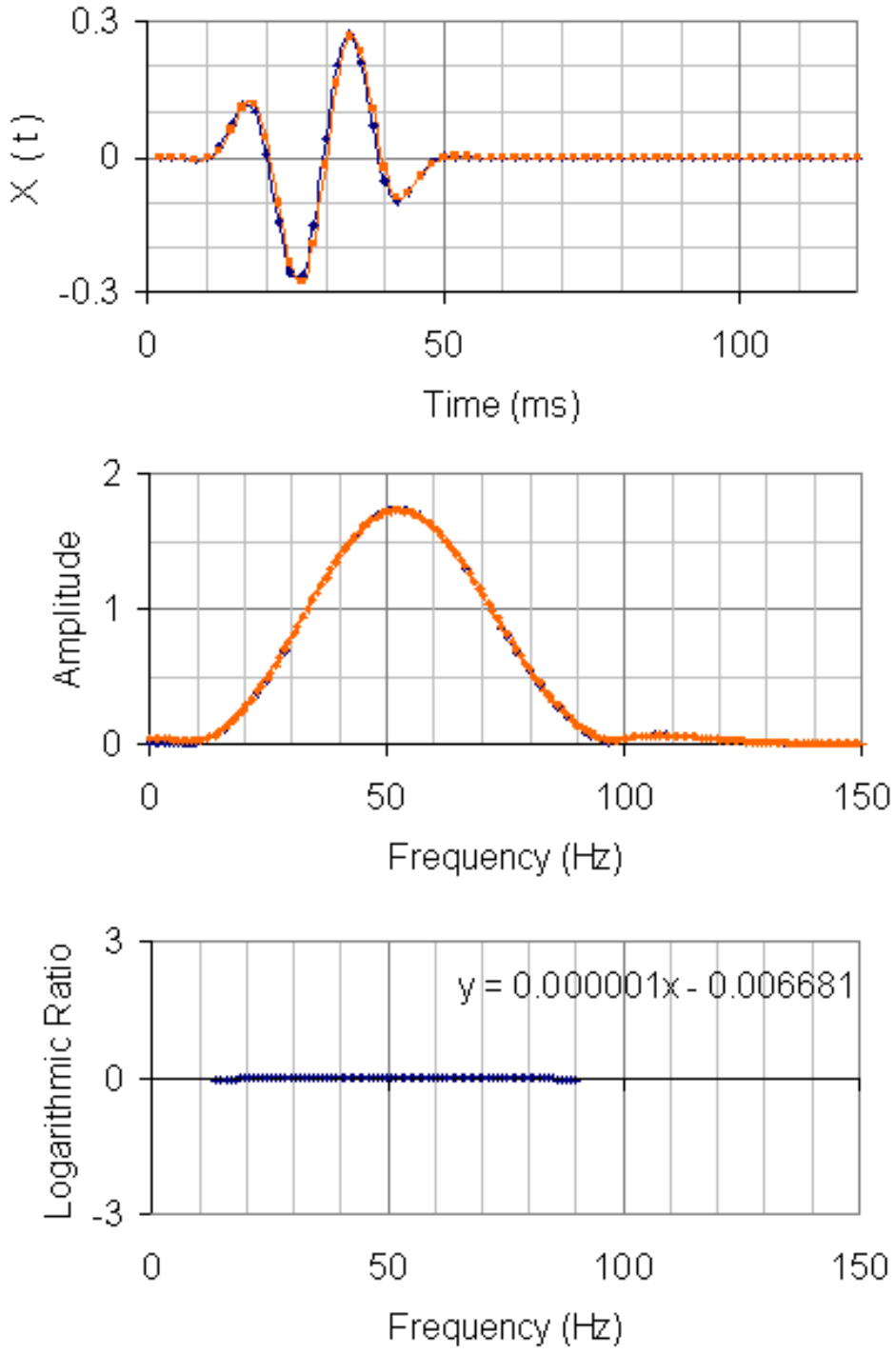

Fig. 3.8. Time signals (top), amplitude spectra (middle) and logarithmic (bottom) ratio plots for the isotropic two layer model without attenuation. Median filter applied to the noise added synthetics ($S/N = 5$). Blue curve in the amplitude spectra represents the amplitude spectrum of the signal recorded at 1 km and the orange curve represents that of the signal recorded at 1.05 km.

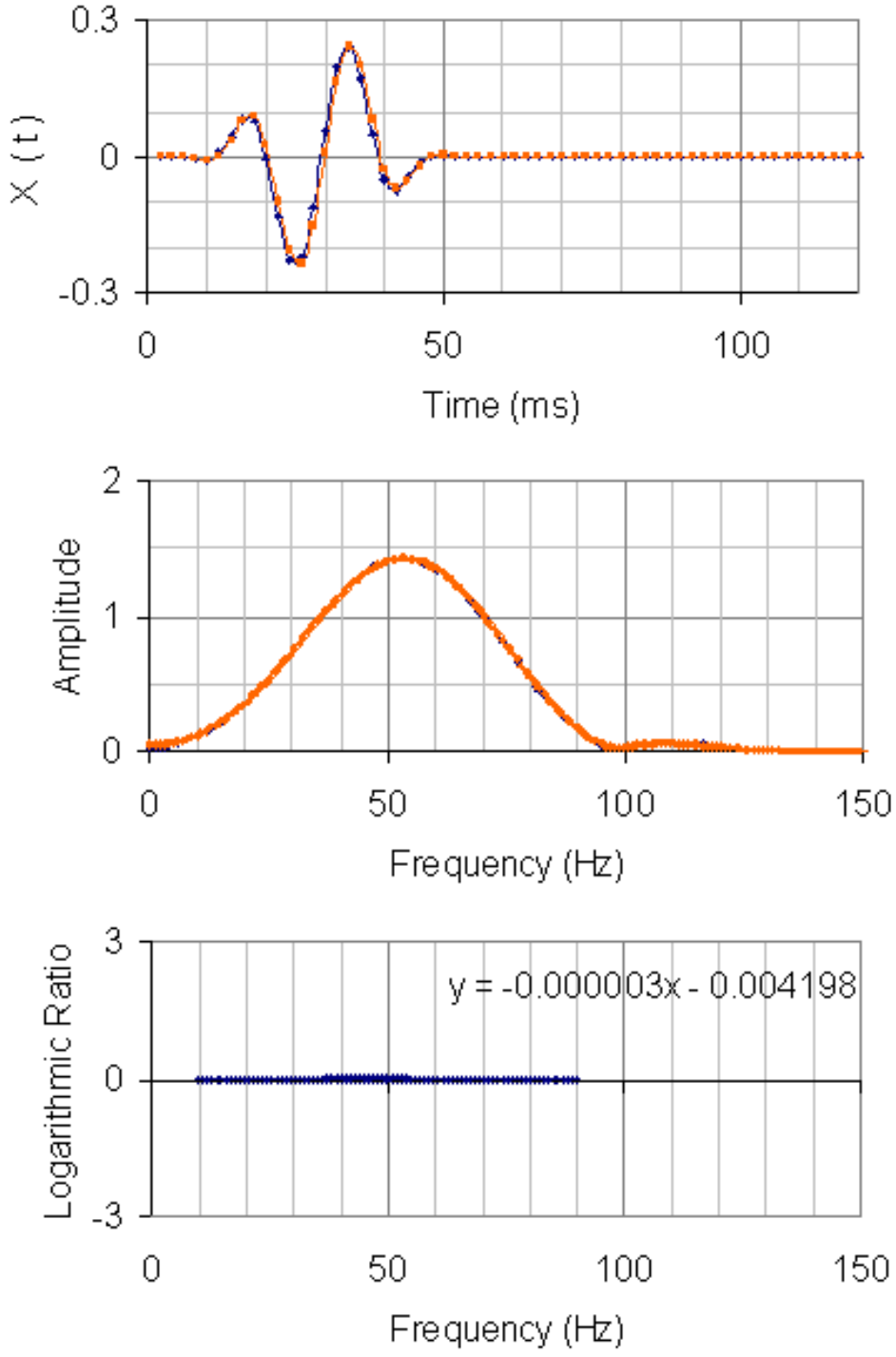

Fig. 3.9. Time signals (top), amplitude spectra (middle) and logarithmic (bottom) ratio plots for the isotropic two layer model without attenuation. Median filter applied to the noise added synthetics ($S/N = 20$). Blue curve in the amplitude spectra represents the amplitude spectrum of the signal recorded at 1 km and the orange curve represents that of the signal recorded at 1.05 km.

and reflecting each time they hit the boundaries. Therefore, the three layer model synthetics at this stage have almost all the possible effects except noise content. To test the SRM, the thin middle layer was given seismic Q of 5 when the top and bottom layers had infinite Q. As mentioned earlier in this chapter, the model synthetics were filtered using median filter.

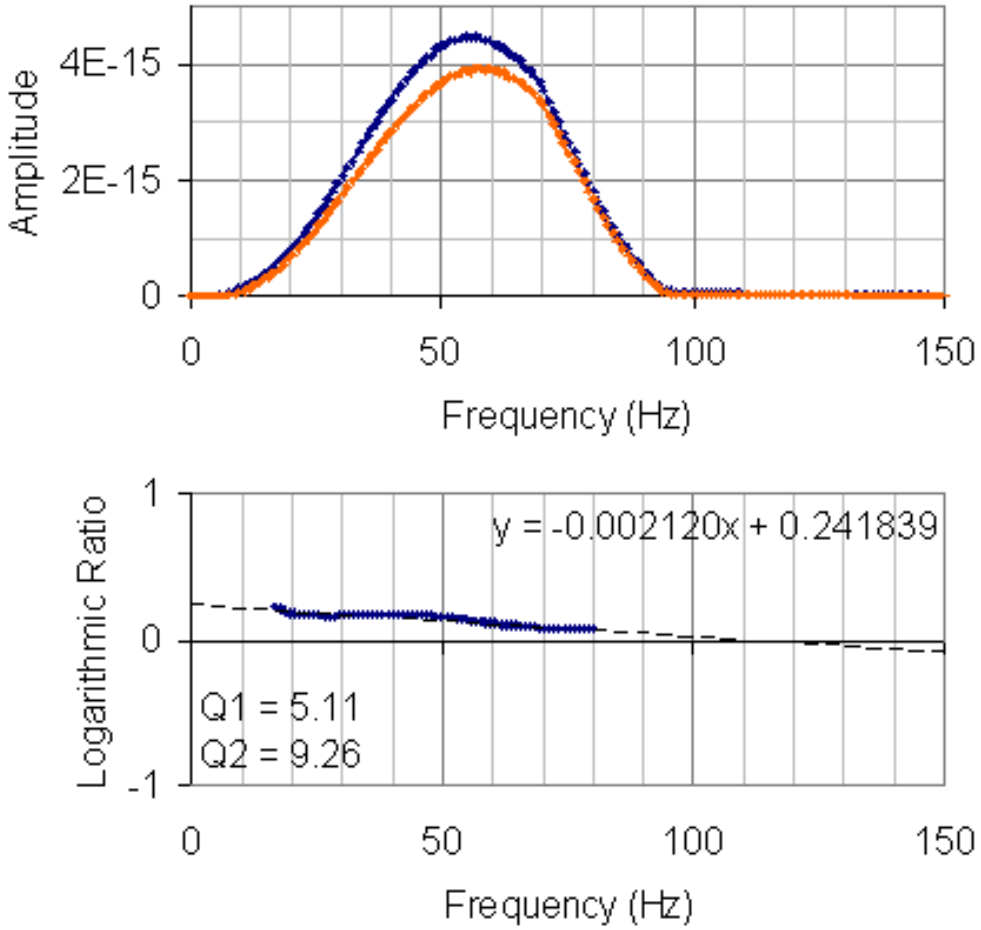

Fig. 3.10. Amplitude spectra (top) and logarithmic ratio (bottom) plots for the three layer model. Blue curve in the amplitude spectra represents the amplitude spectrum of the signal recorded at 2800 ft and the orange curve represents that of the signal recorded at 2850 ft.

Figure 3.10 displays the amplitudes for the receivers at 2800 and 2850 ft and their ratio plot. It is clear that the amplitude spectrum at 2850 ft is considerably lower than that at 2800 ft. The attenuation is expected to be high, and the ratio plot has a significant slope. The complexity of such a model with a thin layer introduces the difficulty in estimating Q because in this depth range there are two different

velocities. However, we can easily test the estimation by using information from both to calculate seismic Q using SRM. Q_1 and Q_2 in Figure 3.10 represent the estimated Q using first and second layer's p-wave velocity respectively. Interestingly, Q_1 is closer to that of the thin layer than Q_2. The amplitude spectra and the ratio plot for the receiver pair 2850-2900 ft is shown in Figure 3.11. Difference in the amplitudes is now much less and the log ratio is nearly constant, implying that the attenuation in the depth range is very small. Q_2 and Q_3 estimates change from 200 to 350 even though the input Q used to calculate synthetics was infinite. Remembering the Q values in nature changing from 10 to 100, these two estimates can be accepted as effectively infinite.

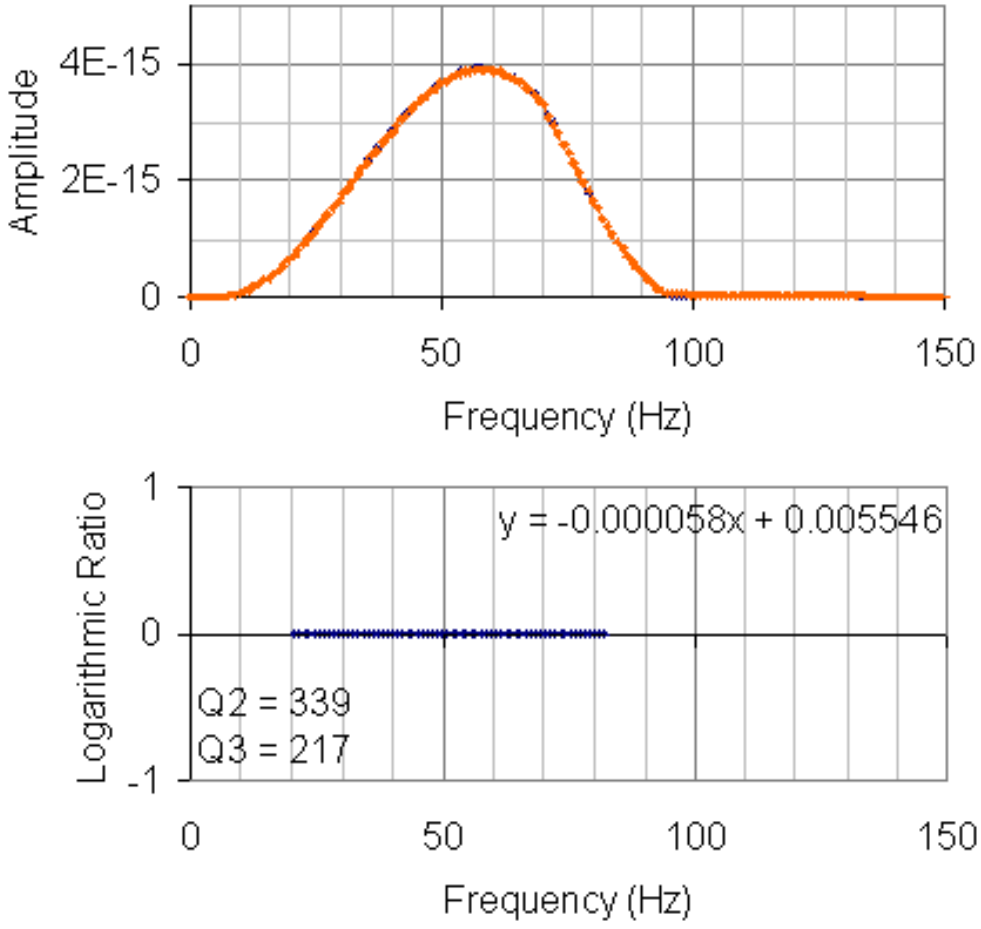

Fig. 3.11. Amplitude spectra (top) and logarithmic ratio (bottom) plots for the three layer model. Blue curve in the amplitude spectra represents the amplitude spectrum of the signal recorded at 2850 ft and the orange curve represents that of the signal recorded at 2900 ft.

The SRM results for the three layer model were satisfying. However, the model synthetics did not have noise interference and SRM should be tested with synthetics having noise content. A new set of synthetics having $S/N = 20$ was calculated for the same geophysical model. The results for the receiver pair 2800-2850 ft are shown in Figure 3.12. The change in the amplitude spectra is obvious but the log ratios show a high slope value. The estimates of seismic Q are similar to those obtained from the noise free synthetics. Again Q_1 seems more likely to represent the thin layer's seismic Q. Note that the error amount in the estimation depends upon how successfully the

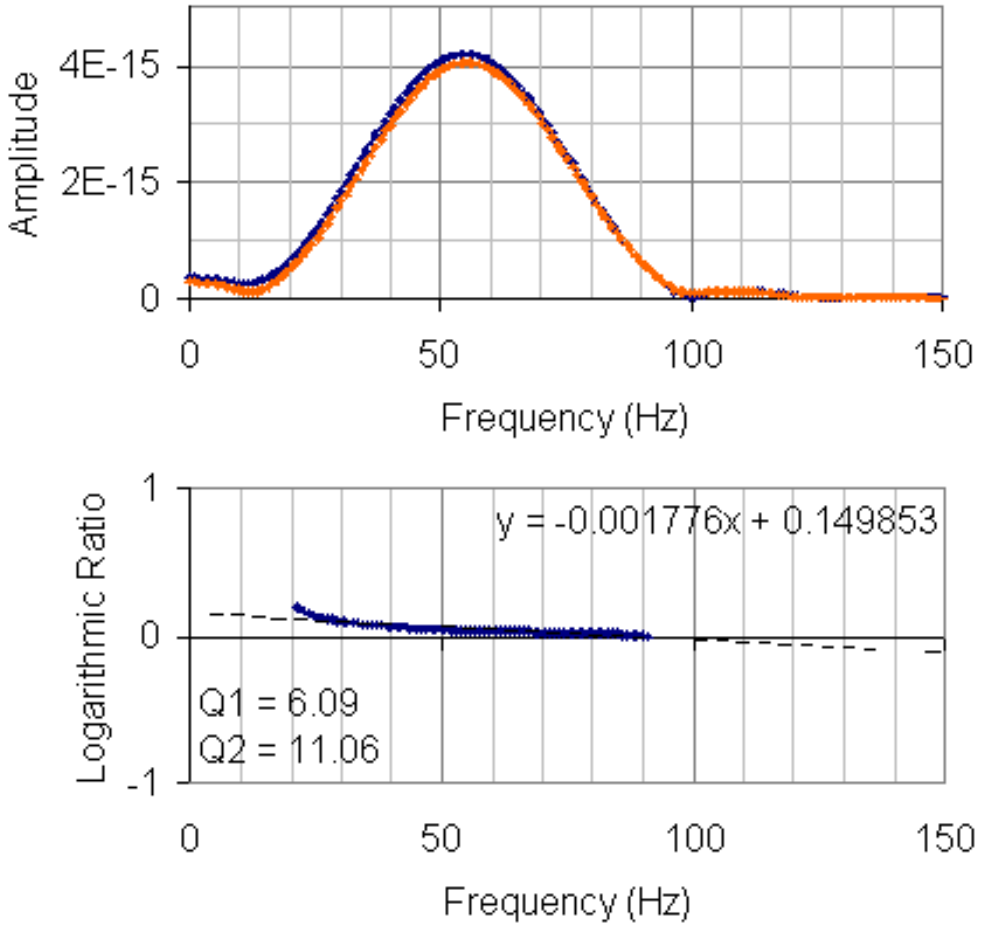

Fig. 3.12. Amplitude spectra (top) and logarithmic ratio (bottom) plots for the three layer model with $S/N = 20$. Blue curve in the amplitude spectra represents the amplitude spectrum of the signal recorded at 2800 ft and the orange curve represents that of the signal recorded at 2850 ft.

median filter applied to the seismograms. Figure 3.13 displays the amplitude spectra for the receivers at 2850 and 2900 ft and their log ratio plots. Q estimation for this

depth interval is again above 200.

In conclusion, SRM has been tested with the synthetics seismograms for different scenarios. The tests explained above proved that SRM is a powerful tool and can be used to successfully estimate attenuation properties of layers even highly attenuative thin layers lying between the receivers. The constraints are that application of median filter to eliminate the interferences such as reflections and noise should be carefully done by choosing the right filter parameters; for example, deciding on the noise band in the frequency range.

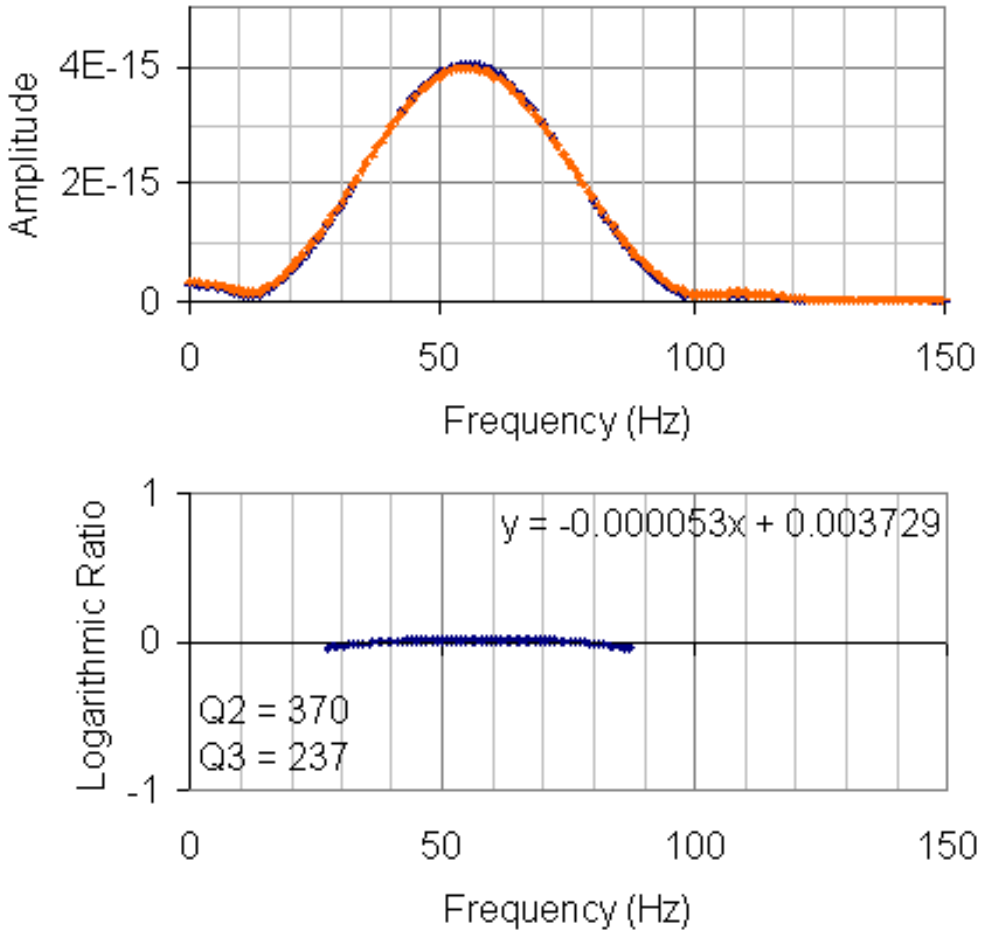

Fig. 3.13. Amplitude spectra (top) and logarithmic ratio (bottom) plots for the three layer model $S/N = 20$. Blue curve in the amplitude spectra represents the amplitude spectrum of the signal recorded at 2850 ft and the orange curve represents that of the signal recorded at 2900 ft.

CHAPTER IV

CUT BANK FIELD VERTICAL SEISMIC PROFILING

DeAngelo and Hardage (2001) recorded VSP data in the south central Cut Bank field. The purpose of recording VSP was to increase the image quality of 3-D seismic survey. Their intent was to obtain velocity information from the VSP itself since there were not enough sonic logs to create the velocity profile of the Cut Bank oil field. Furthermore, tying VSP to 3-D seismic would prove the accuracy of the seismic survey. See Figure 1.1 for the location of VSP well, named 54-8 in the South Central Cut Bank Unit, Glacier County, Montana. Two offsets were chosen for the VSP recordings at 550 (near) and 1100 ft (far). Each recording has 5-components, 2 of which are for time and wavelet correction.

4.1 VSP Velocity Survey

Velocity information was available from the previous works. However, since I had the VSP data loaded in Seislink, I did my own velocity analysis to test the accuracy of the velocity information from previous works. As I mentioned in Chapter II, I had two different first arrival time picking styles. Now I will be explaining why I thought trying different first arrival time picking was a good idea. I named the styles as the first breaks (where the signal energy started) and the first peaks (where the signal reaches its first highest peak (+) energy. A visual demonstration of these approaches can be viewed in Figure 4.1. Testing how accurate the arrival times can easily be achieved by flattening the direct arrivals at picked arrival times. The flattened direct arrivals at the first peaks displayed a better alignment and velocity profile was thought to be satisfactory since it was a big challenge to spot the start of seismic energy in the signals especially at certain depths.

The velocity profile from the previous studies and the two different first arrival time picking styles are displayed on Figure 4.2. I used the near-offset recording to calculate the velocities but velocities from the previous studies were calculated using the available first arrivals times for far-offset VSP. The near and far-offset recordings start at 600 and 1500 ft respectively so the information above these depths assumed

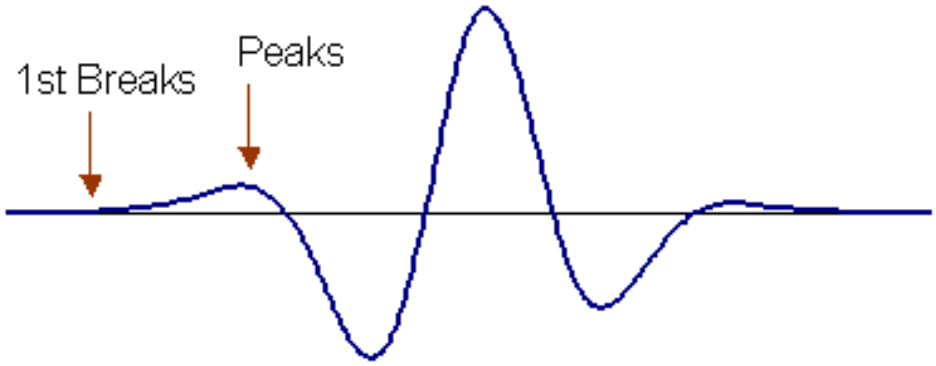

Fig. 4.1. A typical recorded seismic signal and display of the styles that are used in this study for picking first arrival times.

to be the same as it is at these depths for each survey. Comparison of the previous study results with my results reveals that the velocity information may not be that accurate using the far-offset recordings. First of all, there is no clear information for the shallow depths in the previously done results and deeper intervals seem to follow almost the same pattern. Additionally, velocity for the Bentonite zone (2800-2850 ft) seems to be very high ($\sim 18000 ft/s$) for a highly attenuative medium. Results from my methods have similar trends for the shallow depths (600-1800 ft). The first breaks are more unique comparing to the peaks since it displays high velocity jumps along the depth range. However, the peaks seem to be more reliable because the profile is mostly in agreement in the depth range. Erratic nature of first breaks velocity profile is due to interference at the boundaries as reflected events may change the shape of the signal and/or delay the arrival time, which introduce error in the velocities as large jumps in the velocity profiles. Simply, inaccuracy in the first arrival time readings cause wrong velocity calculations. As a result, first arrivals should be carefully chosen since small changes in the first arrival time may result in having totally different velocity structure that may not reflect the formations in the study area. The velocity information from the peaks arrival time picking style is chosen for the study since the signals flattened at first arrivals are in accordance and first peak of a signal is the closest satisfying point to the beginning of the signal. Therefore, the velocity estimates from the peaks arrival times will be considered in this study.

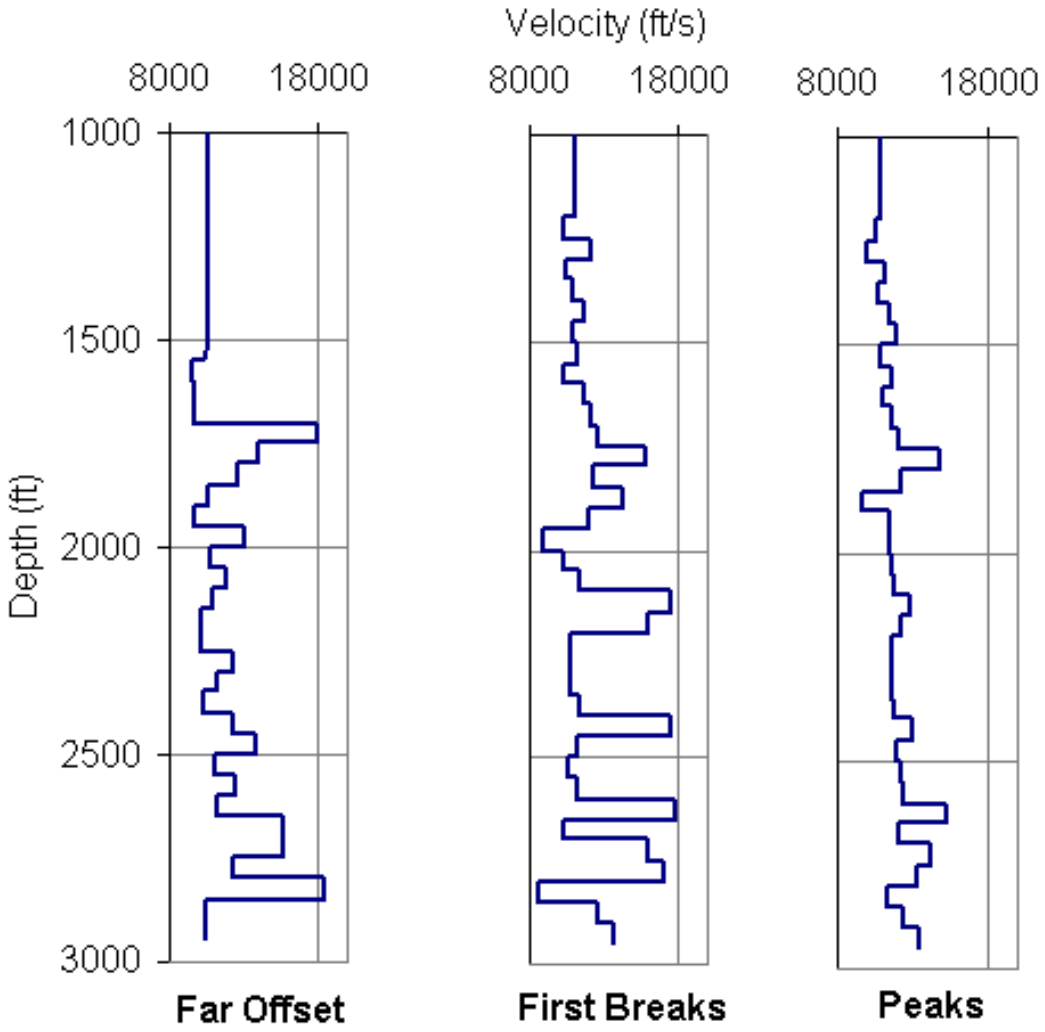

Fig. 4.2. Display of velocity surveys. Far offset VSP results (left), velocity profiles for near offset VSP arrivals at first breaks (middle) and peaks (right).

4.2 Cutbank VSP Noise Analysis

Cut Bank field VSP has its unique noise structure. Figure 4.3 shows the noise spectrum for the field data. The end part of the Cut Bank VSP data was muted at the first breaks and passed through Fourier transform. There are similar patterns in the noise signals that could be generated by a periodical source or there is a source that constantly produces noise. The major energy in the noise accumulates within the 0-50 Hz frequency range. There are a few spikes in the spectrum ($\sim$ 15, 25, and 32 Hz) that state there are individual sources at certain frequencies. These sources

could be anything in the nature such as wind and maybe cause by the railroad track and Cut Bank creek nearby the study area. Also note that noise content of the Cut Bank field VSP data seems to have decreasing trend, which explains that there is no anomalous noise sources in the subsurface in the area.

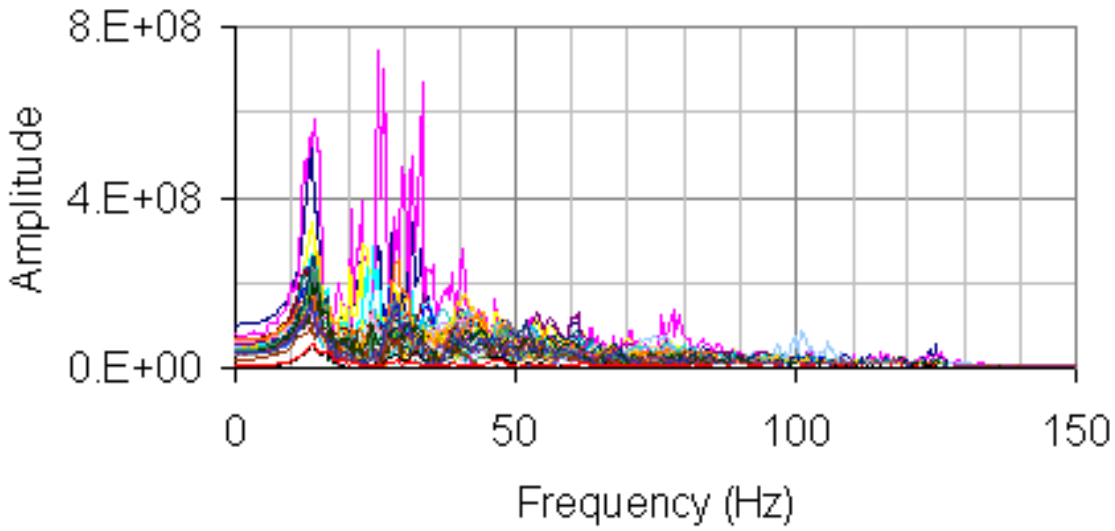

Fig. 4.3. Noise spectrum of Cut Bank field VSP data. Direct arrivals and reflected events are muted.

4.3 Processing Cut Bank Field VSP

The spectral ratios method (SRM) was previously discussed and tested in Chapter II. The available information for the Cut Bank field data that could be used in parallel to this study is a couple of 3-D seismic lines and gamma-ray and density logs for the well # 54-8 as discussed in the Chapter I. In this section, application of SRM to the Cutbank field VSP data will be discussed. Noise presence and also lack of sonic logs is a big challenge to process the Cut Bank field VSP data. The main goal of the study is to focus on the thin Bentonite layer, which could be successfully achieved by analyzing the seismic amplitudes of the field VSP data. Latter the two available well logs can affirm the results, maybe not with Bentonite's precise depth but with the depth interval where the Bentonite layer resides.

The importance and advantages of using median filter were previously discussed in Chapter II. The VSP recorded with 550 ft offset is chosen to proceed with the study since SRM assumes that seismic signals travel vertically. Therefore, using only

the vertical component of Cut Bank field VSP is enough. A brief look at the field VSP, there are doubled recordings at the same depth and some of these doubled futures had reverse polarity. I also noted a constant time shift of 100 ms from the fifth component for time correction. The extra traces were eliminated and 100 ms time shift was applied to the data. See Figure 4.4.

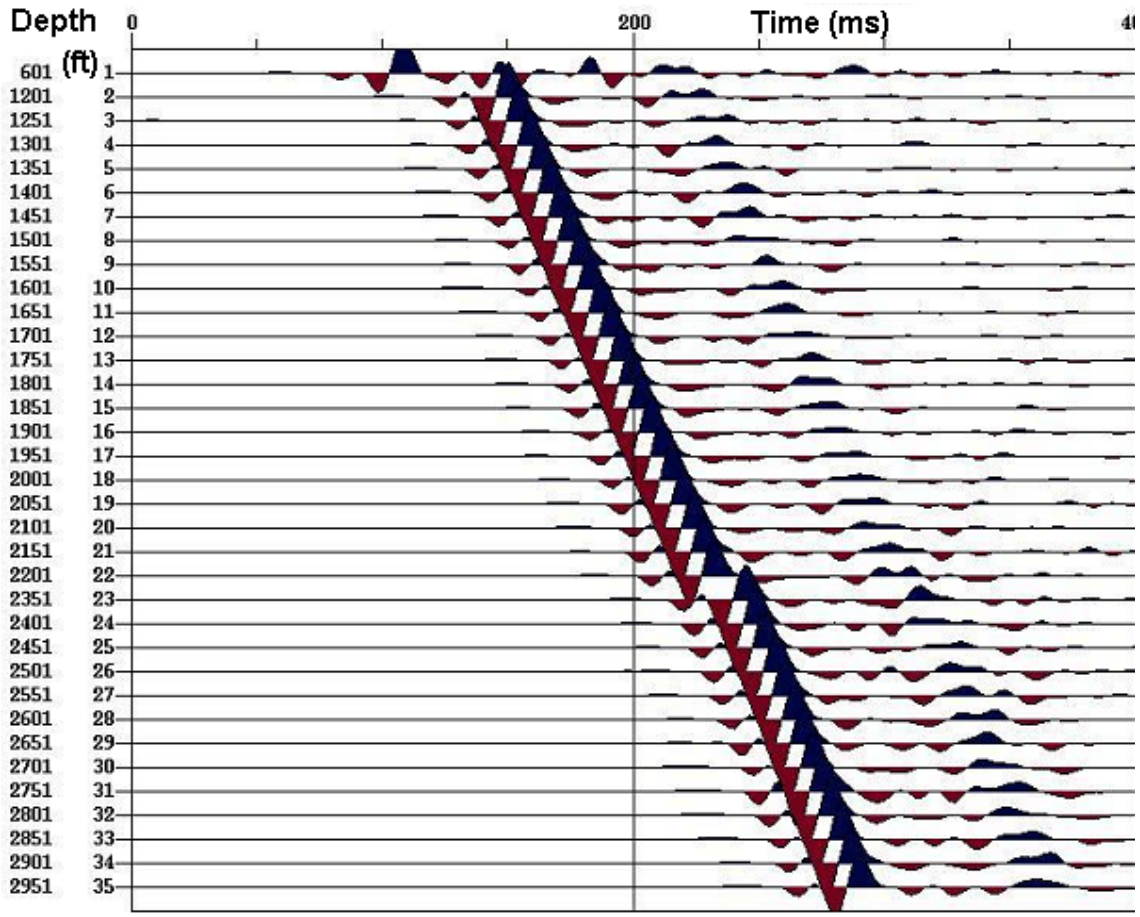

Fig. 4.4. Display of vertical component from Cut Bank field VSP data.

4.4 Median Filter Application and VSP to Surface Seismic Tie

The idea of tying VSP to seismic led me to apply median filter to the Cut Bank VSP. As we know we can use median filter to separate the reflected events from transmitted events. Once median filter applied we can view the reflections and stack them using Seislink. Figure 4.5 displays the reflected events and the stack of these events on

the right. Later the stacked traces were aligned to match the scale of seismic line where the VSP well # 54-8 is located. See Figure 4.6 for seismic to VSP tie of Cut Bank field. Tie of VSP with surface seismic is quite successful especially around the reservoir area. Note that there is about 40 ms time difference between the surveys, which is a result of different datum levels.

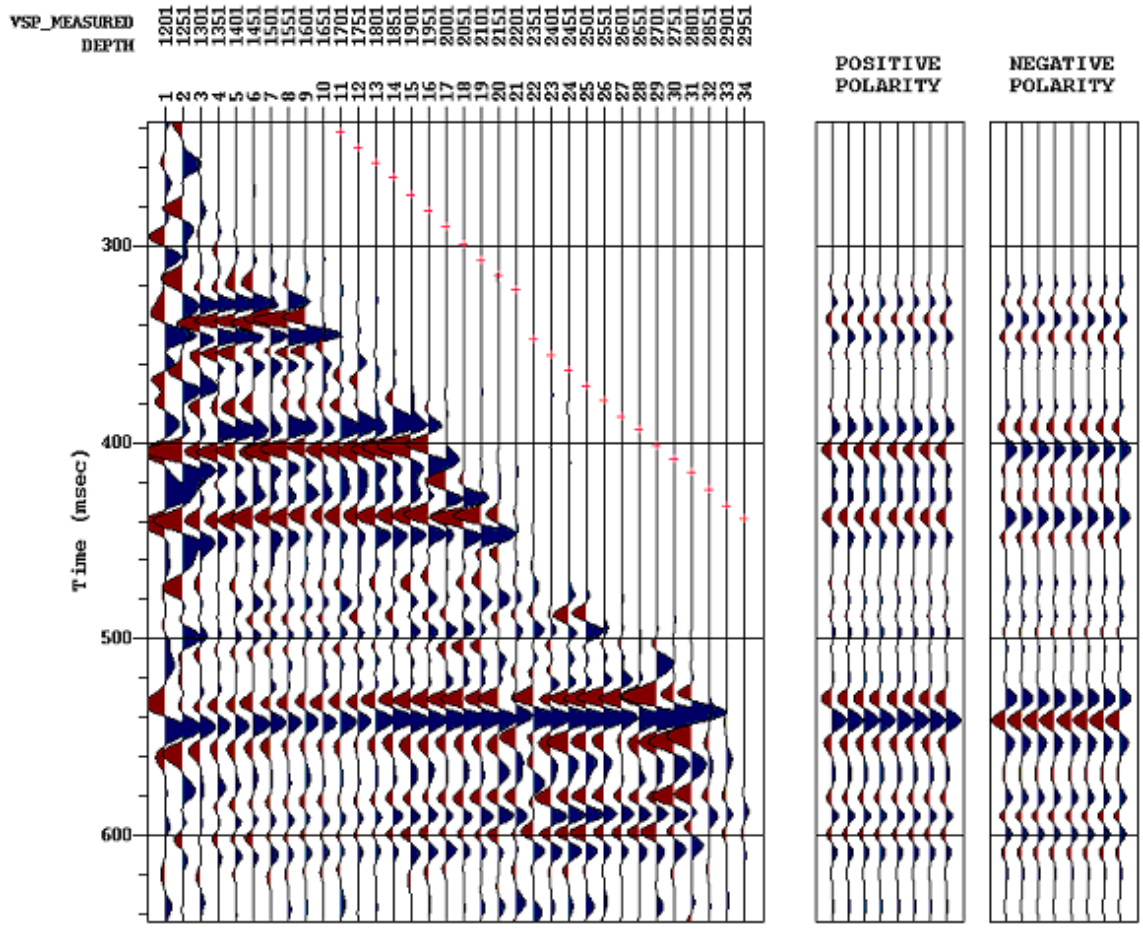

Fig. 4.5. Reflected events from Cut Bank field filtered by median filter (left) and the stack of these reflected events (right).

4.5 Application of SRM to the Cut Bank VSP Data

One good advantage of applying median filter is that once we separate the up-going waves from down-going waves, we can use either of these data sets for our future processes. Evidently, we now have direct arrivals on hand since median filter was

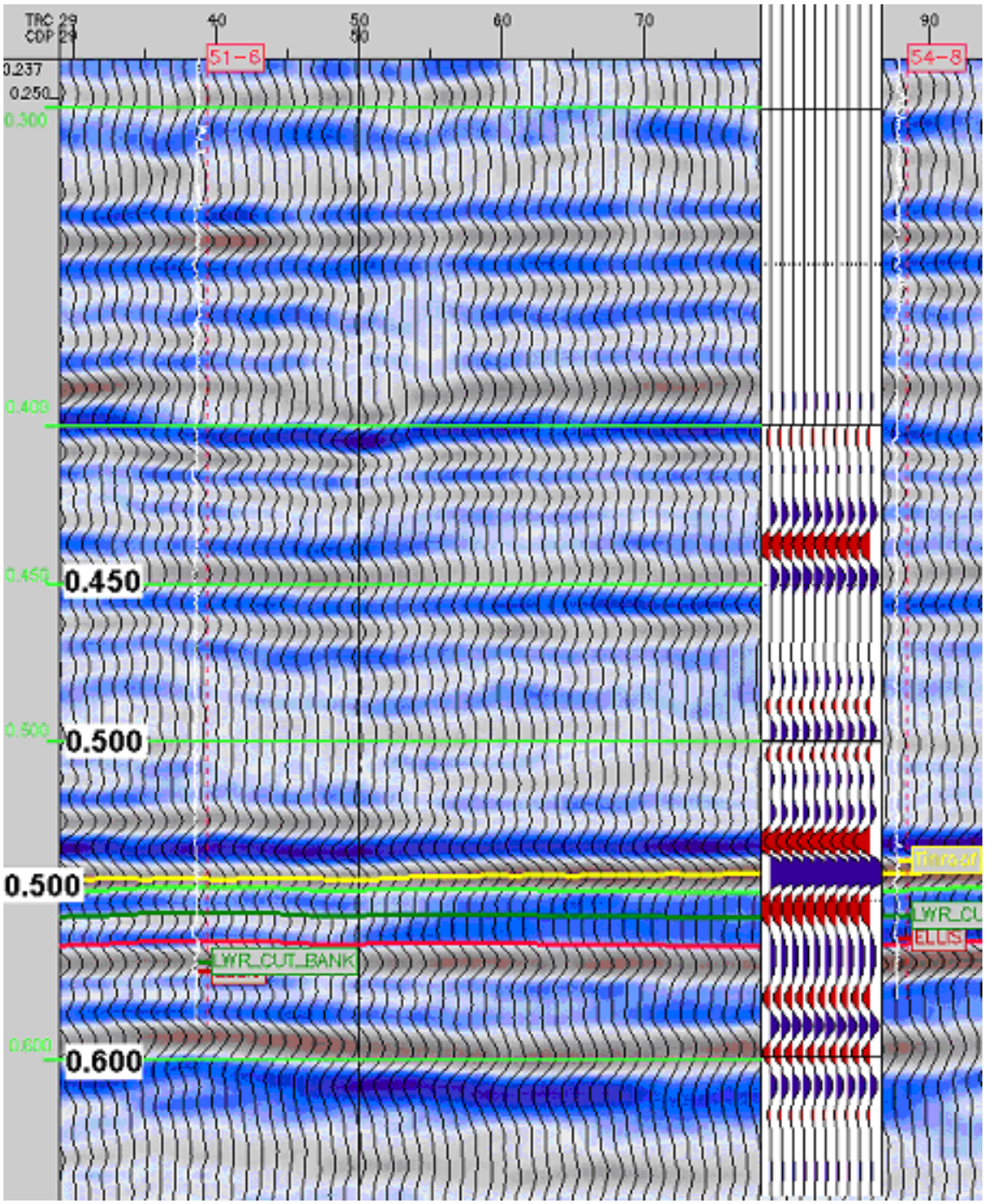

Fig. 4.6. Display of Cut Bank VSP tie to 3-D surface seismic.

applied to the Cut Bank VSP. Now that we have the direct arrivals ready for SRM processing, we can move on to estimating seismic Q from the Cut Bank VSP.

4.5.1 Choosing Frequency Range

In this chapter, I have mentioned the factors that affect the accuracy of Q estimation from SRM. However, choosing the frequency band for Q estimation has not been explained, yet. Chosen frequency band is very important because the amplitude spectra do not always have information within the whole frequency range. This is because the source signal may not carry all the frequencies itself or even it did, information on some of these frequencies might be either interfered by noise or attenuated during propagation. The major ambiguity is how to determine which frequencies actually carry the source signature or which part of the amplitude spectra has useful information.

Before analyzing the frequency band, lets examine the Q estimation results for Cut Bank VSP data. Figure 4.7 is a display of Q estimation for the same data set but frequency range used for Figure 4.7 (left) is 0-150 Hz and that for Figure 4.7 (right) is 0-250 Hz. Shaded areas on the plots refer to the intervals where amplitude spectra did not fit the SRM model. These depth intervals yielded no Q estimation and were excluded from the Q estimations. There is quite a bit unknown Q values on both of the plots but the major point is that Q estimations from both frequency ranges do not match. This result raises the importance of choosing the right frequency range for seismic Q analysis.

How do we choose the right frequency range? One possibility is very simple and lies in the amplitude spectrum itself. The amplitude spectrum does not always contain seismic energy itself. It also includes effects of other signals and noise. To be able to correctly analyze attenuation; we need to omit noise content and possible interference from our data. Finding the high and low ends of the frequency range will help resolve the interference and noise effects from the spectrum. Example amplitude spectra from the receiver pair 1500-1550 ft are shown in Figure 4.8. Assumptions for the SRM are that the seismic energy attenuates downward in to the earth and that the propagation direction is vertical. Knowing these limits, we can assume that high and low end of the frequency range will be wherever the amplitude at the shallower depth is larger than or equal to that at the bottom depth. The low end of the frequency

range is obviously zero since both spectra do not intersect at the low frequencies in

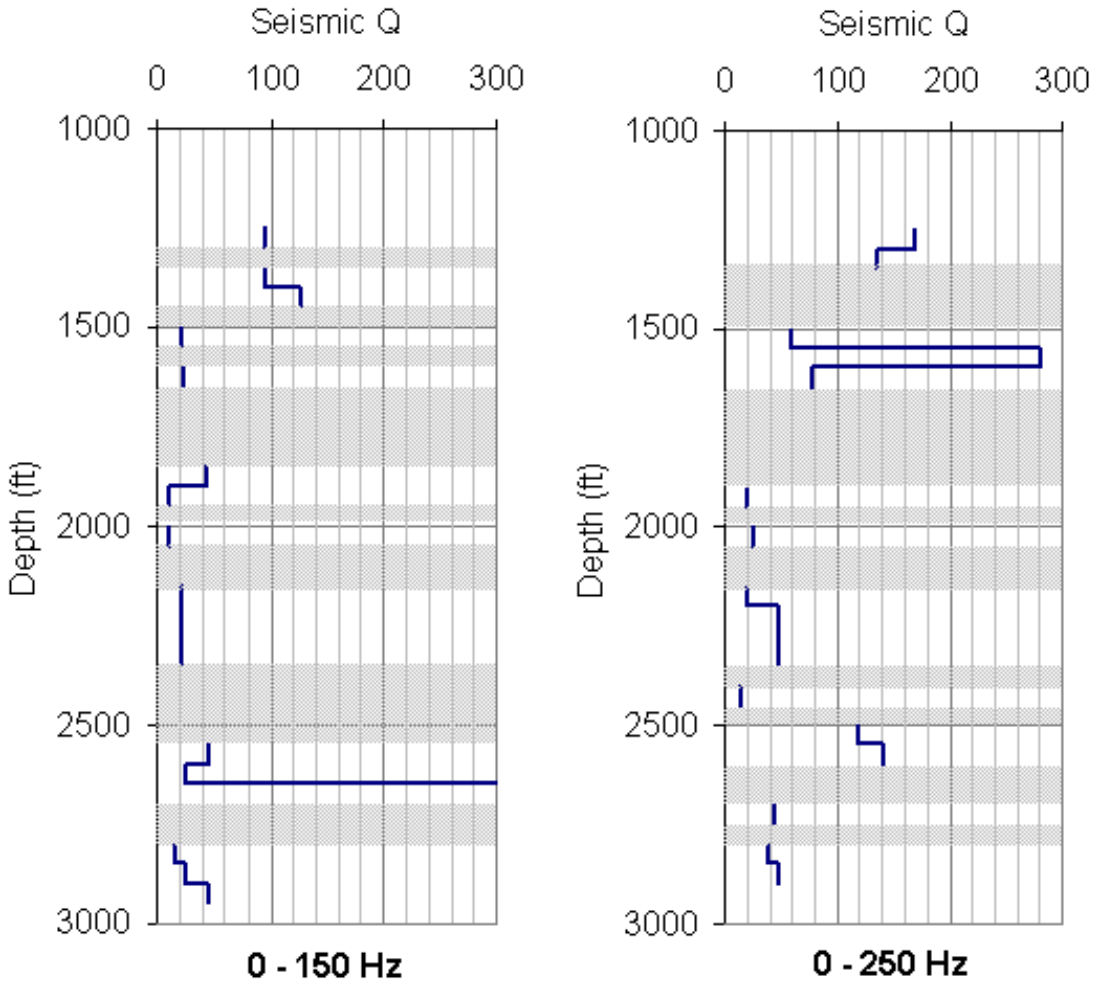

Fig. 4.7. Display of effects of chosen frequency band on Q estimations. Q estimation for Cut Bank VSP data: chosen frequency range 0-150 Hz (left) and chosen frequency range 0-250 Hz (right).

Figure 4.8. The high end of the range is too hard to find, either because right after 100 Hz the shallower spectrum equals to the deeper one. The chosen frequency range for this depth interval will be 0-100 Hz. Figure 4.9 shows the logarithmic ratio plot for the depth interval 1500-1550 ft. Having logarithmic ratios as shallow over deep receiver result in negative slope and gives reasonable Q value. Using SRM, estimated seismic Q for this receiver pair is 12.48.

There are special cases where the above rule to choose frequency fails. For example, the receiver pair at 1700 and 1750 ft has to be examined closely. The

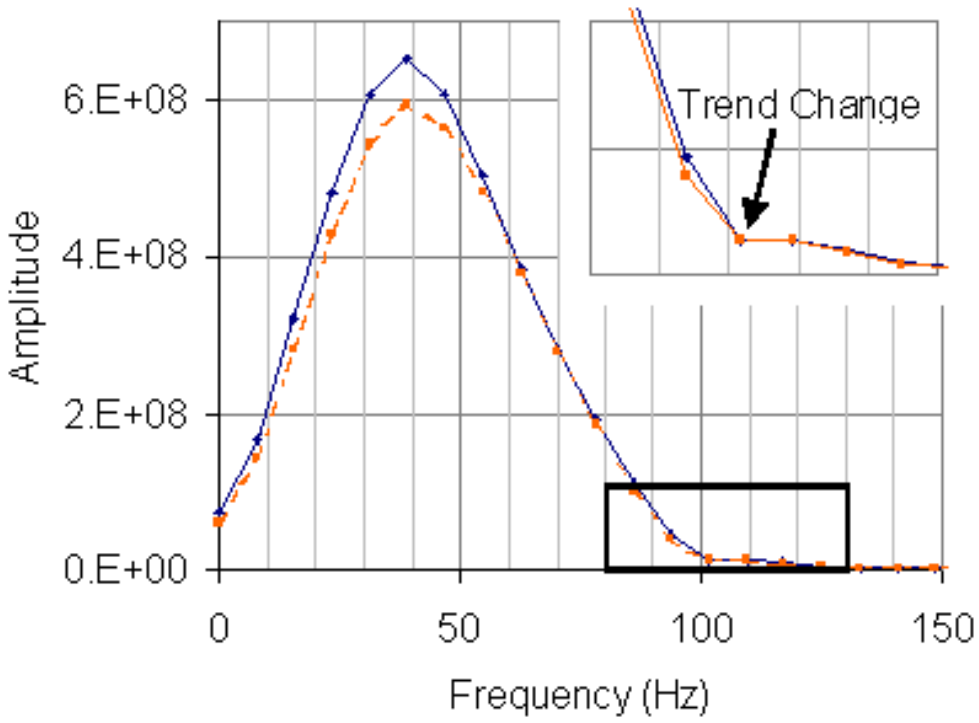

Fig. 4.8. Amplitude spectrum of seismic signals recorded at 1500 (blue) and 1550 ft (orange).

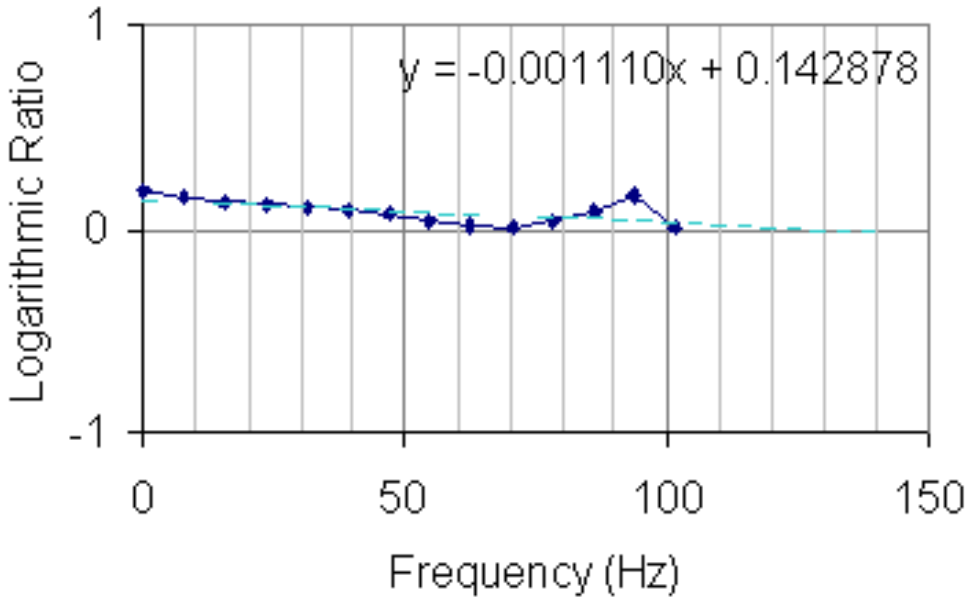

Fig. 4.9. Logarithmic ratio plot of the receiver pair at 1500 and 1550 ft.

amplitude spectra for this pair are shown in Figure 4.10. The frequency range is 0-100 Hz with the help of the amplitude based frequency range but the ratio plot has a positive slope, which means a negative Q estimation. Apparently, there are some other effects in the spectrum. Taking a close look at the spectra between 70 and 85 Hz in Figure 4.10, we can easily see that the difference between the spectra is constant i.e. there is an apparent interference in the spectra. The source of the interference can be a processing effect or the filter could not suppress the noise in that range. What we can do is to omit these frequencies from the Q estimation. Figure 4.11 has both ratio plots for the chosen frequency range before and after that range omitted. As it is clear, now the slope of the ratio curve is negative and we have positive (logical) seismic Q value.

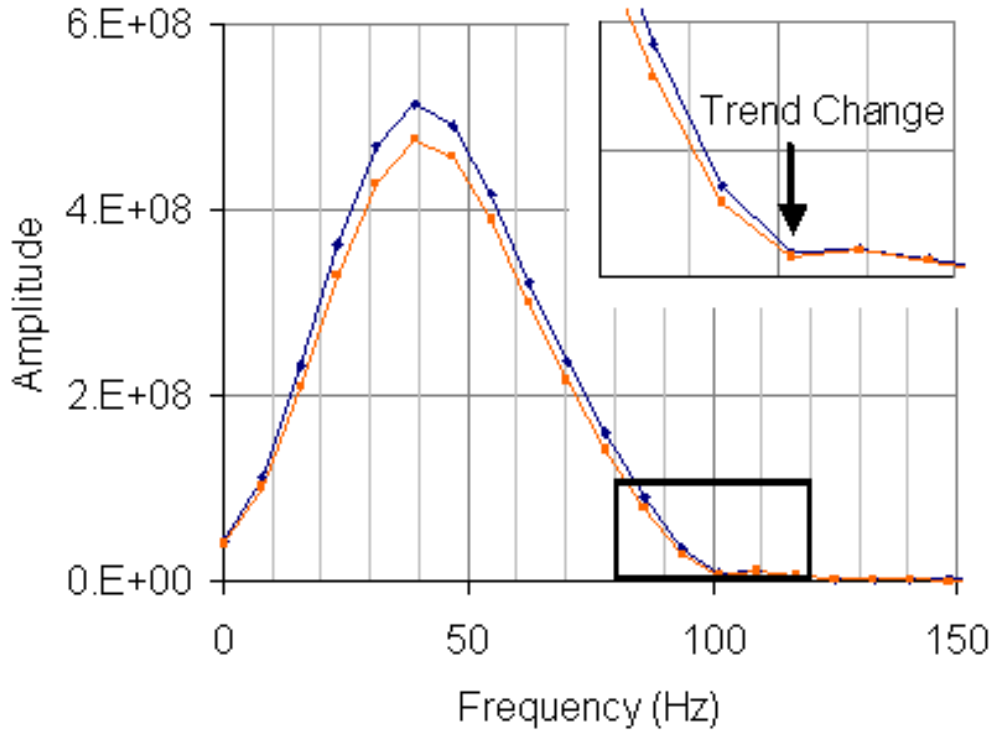

Fig. 4.10. Amplitude spectrum of seismic signals recorded at 1700 (blue) and 1750 ft (orange).

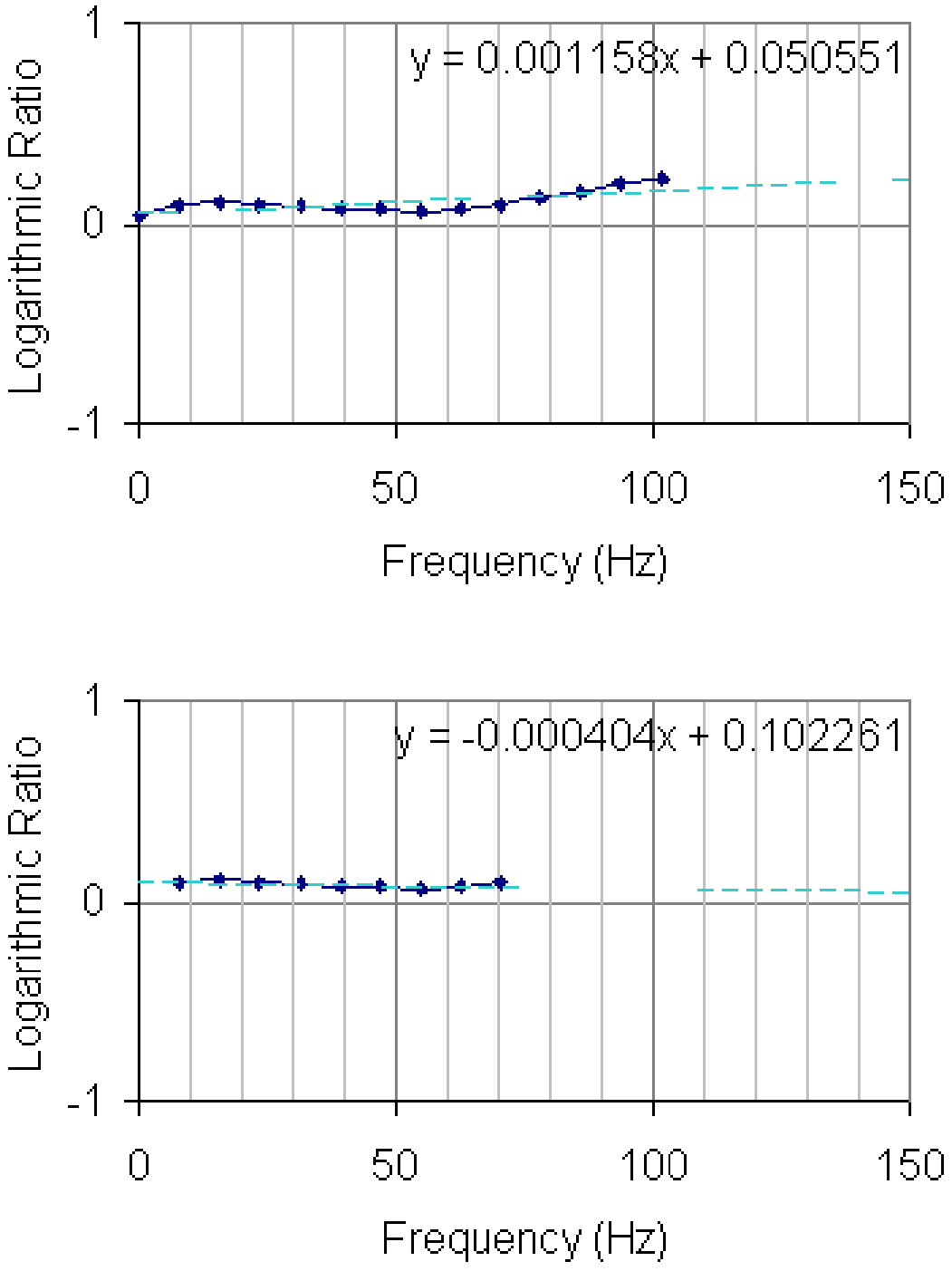

Fig. 4.11. Logarithmic ratio plot of the receiver pair at 1700 and 1750 ft for two different frequency ranges of analysis.

4.5.2 Q Estimation from SRM for Cut Bank Field VSP Data

After examining amplitudes and characterizing how to choose the frequency range, seismic Q values using SRM were estimated for the Cut Bank field VSP data. Estimated Q values are displayed in Figure 4.12. The plot on the left hand side is the large scale and the one on the right hand side is the smaller scale of the same Q results for the Cut Bank data. A skecth of the geological section obtained from well logs is also given in Figure 4.12. Shaded areas in the Q plots indicate negative Q results, which are omitted for display purposes because there can not be a negative Q value in nature. Applying amplitude based frequency range noticeably improved the Q results. The number of negative estimations in 5 depth intervals as opposed to more than 10 in the previous frequency range tests. Bentonite zone 2800-2850 ft displays a very low Q, approximately 5. Interestingly there are other high attenuative zones in the depth range from 1750 to 2200 ft, lower portion of Colorado Shale. Estimates for the other depths are fairly scattered between 15 to a few hundreds. Furthermore,

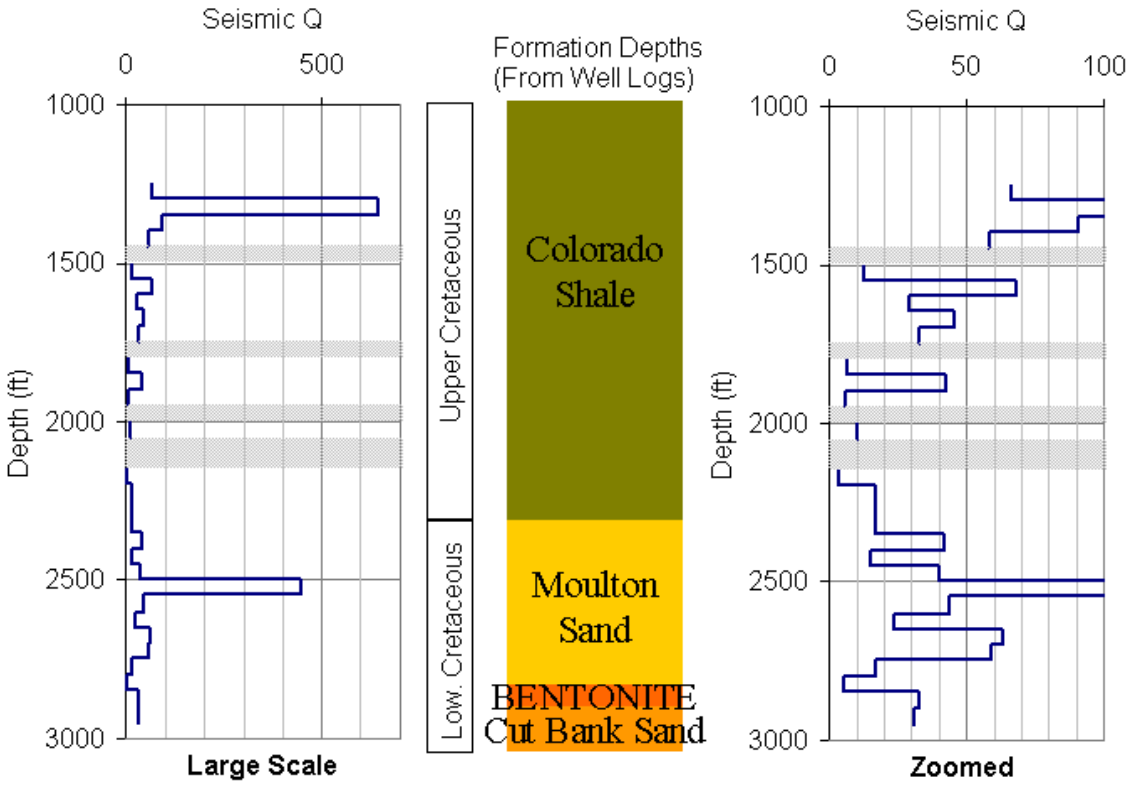

Fig. 4.12. Q estimation for Cut Bank VSP data using amplitude based chosen frequency range for SRM method.

we can clearly note that the depth of the Bentonite layer from well logs lies within the estimated low Q depth interval.

4.6 Analysis of Seismic Amplitudes Above and Below the Bentonite Layer

Understanding the amplitude behavior is important when studying seismic Q. In this section, amplitude spectra from the depths above and below Bentonite layer will be examined and interpreted. Spectra are given in Figure 4.13. Throughout the study how and how much attenuation affected seismic amplitudes were mentioned. I hereby summarize a few observations based the information given in this study. The amplitude spectrum at depth 2800 ft in Figure 4.13 clearly confirms the decay in the seismic energy as it is ten-times higher than the spectra below it. Note that the Bentonite layer is highly attenuative and the huge energy decay from 2800 to 2850 ft confirms this knowledge. The shift in the highest peak amplitude towards the low frequencies is also another factor caused by seismic wave attenuation. Overall, non-zero amplitudes below 2800 ft have narrower frequency range and implements that amplitude loss was proportional within the frequency band of the seismic signals. This is similar to model results presented in section 3.6 as well, providing additional confirmation of this interpretation.

Briefly, the seismic amplitude remains low after passing the highly attenuative zone (Bentonite layer), which states that seismic wave attenuation persists. Seismic wave amplitude can not be recovered after attenuation even if it bounces back from the bottom of this layer and travels upward into the low attenuative medium. As a result, just looking at the amplitude spectra one can have some ideas about in what kind of structures the seismic waves are traveling or if certain depth intervals require more careful processing or if special attention needs to be considered at certain receivers.

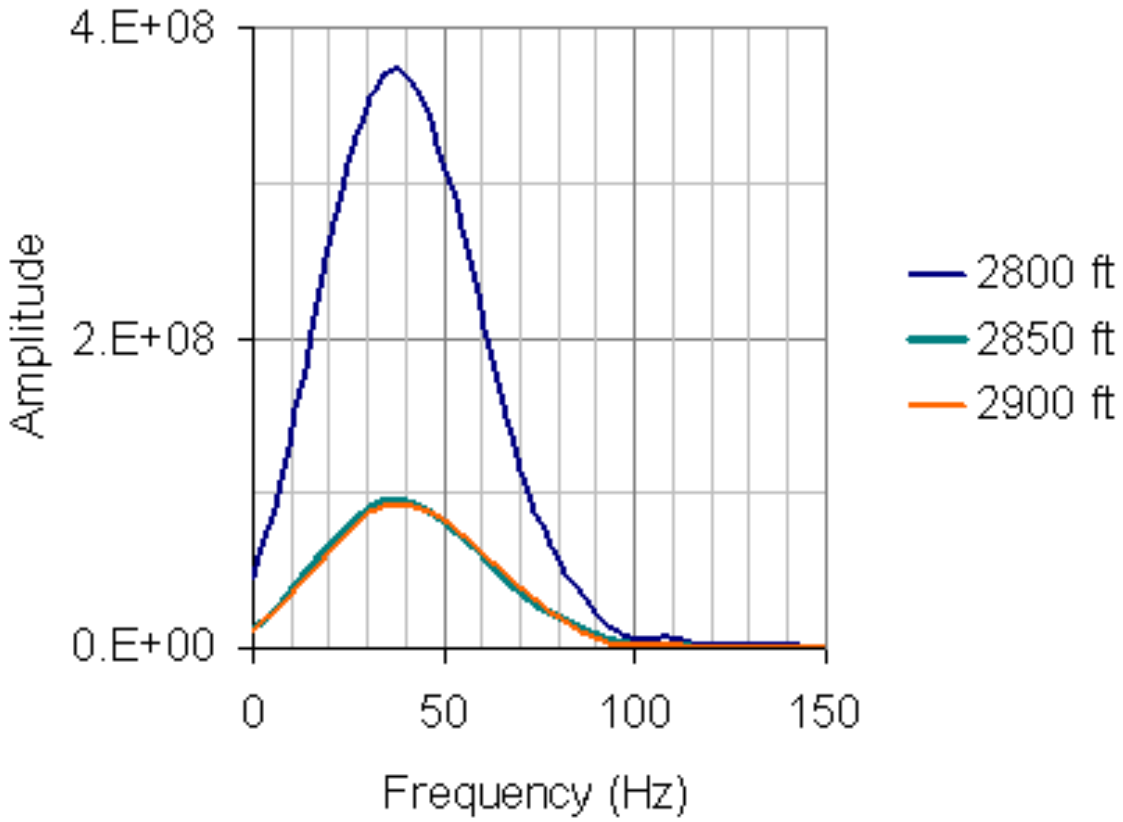

Fig. 4.13. Amplitude spectra for the receivers at depths 2800, 2850, and 2900 ft.

CHAPTER V

CONCLUSIONS

5.1 Conclusions

Seismic Q analysis was applied to the Cut Bank field VSP data. Careful application of processing techniques to the Cut Bank field VSP data yielded valuable results. SRM tests were successfully made using synthetic seismograms computed for two different geophysical models and attenuation mechanisms. The seismic Q estimations from the field data is quite satisfying even though a few of the receiver pairs' amplitude spectra did not fit the SRM, resulting in no Q computation. There are also a couple of receiver pairs that fit the SRM but produced unlikely Q estimations. The rest of the depths has reasonable Q values and proved that application of SRM to the Cut Bank VSP was satisfactory. Estimated Q for the zone that includes Bentonite layer is noticeably low at about 5, which represents a highly attenuative structure. Highly attenuative structures like Bentonite need to be taken seriously for better analyzing of seismic data. It is well known that thin layers constructively affect seismic signals. Constructive nature comes from reflections and multiples within the thin layer that add up on direct arrivals with some delay and change their content. In addition, if this thin layer is highly attenuative, understanding and eliminating these effects from our recording will become a big challenge. Indeed, we need to process seismic data more carefully and accordingly.

Signal characteristics are obviously affected by attenuation as they become broader in time and narrower in frequency domain. Having a thin high attenuation layer above the reservoir sequence results in inseparable reflections since the reservoir sand units in the area are also considerably thin. To be able to separate each reflection from each individual layer, we need to use much smaller wavelength (1/3 of the targeted layer thickness). Measuring the variation in the reflection characteristics for the Cut Bank sand units might be a future study.

In conclusion, the spectral ratios method used in this study is a quite successful technique. The results from the SRM exceeded our expectations, as Bentonite layer is now believed to be very attenuative medium ($Q = 4$). In the introduction section of

this thesis, I introduced a few questions as how the research would proceed. I believe these questions are fairly answered and this study served its purpose.

REFERENCES

Balch, A. H., Lee, M. W., Miller, J. J., and Ryder, R. T., 1982, The use of vertical seismic profiles in seismic investigations: Geophysics, **47**, 906-918.

Bartram, J. G. and Erdmann, C. E., 1933, Natural gas in Montana: MSR Exploration.

Biot, M. A., 1956a, Theory of propagation of elastic waves in a fluid saturated porous solid. II. Low frequency range: J. Acoust. Soc. Am., **28**, 169-178.

Biot, M. A., 1956b, Theory of propagation of elastic waves in a fluid saturated porous solid. II. High frequency range: J. Acoust. Soc. Am., **28**, 179-181.

DeAngelo, M. V. and Hardage, B. A., 2001, Using 3-D seismic coherency and stratal surfaces to optimize redevelopment of waterflooded reservoirs, Cut Bank field, Montana: Burea of Economic Geology, Geological Circular 01-1.

Hardage, B. A., 1995, 3-D seismic thin-bed imaging: The University of Texas at Austin, Bureau of Economic Geology, technical summary conducted for the Gas Research Institute, U.S. Department of Energy, and the State of Texas, GRI-95/0188.

Johnston, D. H. and Toksoz, M. N., 1980, Ultrasonic P and S wave attenuation in dry and saturated rocks under pressure: J. Geophys. Res., **85**, 925.

Klimentos, T. and McCann, C., 1990, Relationships among compressional wave attenuation, porosity, clay content, and permeability in sandstones: Geophysics, **55**, 998-1014.

Kuster, G. T. and Toksoz, M. N., 1974, Velocity and attenuation of seismic waves in two phase media. Part 1; Theoretical formulations: Geophysics, **39**, 587-606.

Mavko, G. M. and Nur, A., 1975, Melt squirt in the asthenosphere: J. Geophys. Res., **80**, 1444-1448.

Mavko, G. M. and Nur, A., 1979, Wave attenuation in partially saturated rocks: Geophysics, **44**, 161-178.

Romine, T. B., 1929, Oil fields structure of Sweetgrass Arch, Montana: MSR Exploration, personal communication.

Shaw, F., Worthington, M. H., Andersen, M. S., and Petersen, U. K., 2004, A study of seismic attenuation in basalt using VSP data from a Faroe Islands borehole: EAGE 66th Conference and Exhibition-Paris, France, http://www.basaltphysics.net/shaw_2004_eage_p015.pdf.

Solomon, S. C., 1973, Shear wave attenuation and melting beneath the Mid-Atlantic Ridge: J. Geophys. Res., **78**, 6044-6059.

Stoll, R. D. and Bryan, G. M., 1970, Wave attenuation in saturated sediments: J. Acoust. Soc. Am., **47**, 1440-1447.

Toksoz, M. N., Johnston, D. H., and Timur, A., 1979, Attenuation of seismic waves in dry and saturated rocks. I. Laboratory measurements: Geophysics, **44**, 515-528.

Walsh J. B., 1966, Seismic wave attenuation in rock due to friction: J. Geophys. Res., **71**, 3532-3536.

Walsh J. B., 1969, New analysis of attenuation in partially melted rock: J. Geophys. Res., **74**, 4333-4337.

Weimer R. J. and Tillman R. W., 1980, Sandstone reservoirs: SPE 10009.

Winkler, K. and Nur A., 1979, Pore fluids and seismic attenuation in rocks: Geophys. Res. Lett., **6**, 1-4.

VITA

Name: Necdet Karakurt

Address: Department Of Geology & Geophysics, Texas A&M University, College Station, TX 77843-3115

E-mail Address: karakurt98@hotmail.com

Education: B.S., Geophysical Engineering, Istanbul Technical University, 1995
M.S., Geophysics, Texas A&M University, 2005